Aus dem Centrum für Schlaganfallforschung Berlin der Medizinischen Fakultät der Charité – Universitätsmedizin Berlin

DISSERTATION

Improved assessment of hypoperfusion, blood-brain barrier disruption, and ischemic cellular damage in stroke patients using magnetic resonance imaging

zur Erlangung des akademischen Grades

Medical Doctor - Doctor of Philosophy (MD/PhD)

vorgelegt der Medizinischen Fakultät

Charité – Universitätsmedizin Berlin

von

Ahmed Abdelrahim Ahmed Khalil

aus Dschidda, Saudi-Arabien

Datum der Promotion:

07.12.2018

Table of contents

1 Summary 3
1.1 Abstract (English) 3
1.2 Abstract (deutsch) 4
1.3 Introduction 5
1.4 Objectives 9
1.5 Methods 9
1.6 Results 15
1.7 Discussion 18
1.8 Bibliography 21
2 Affidavit 27
3 Declaration of contribution to the publications 28
4 Print versions of the selected publications 29
4.1 Publication 1 29
4.2 Publication 2 41
4.3 Publication 3 54
5 Curriculum Vitae 68
6 Complete List of Publications 71
6.1 Peer-reviewed original research articles 71
6.2 Book chapters 71
6.3 Preprints 72
6.4 Selected conference abstracts 72
7 Acknowledgments 75

1 Summary

1.1 Abstract (English)

Introduction

Emerging magnetic resonance imaging (MRI) techniques can potentially improve clinical decision-making in acute stroke. First, however, these techniques need to be investigated in a routine clinical setting and their use thoroughly validated by comparing them to established methods and relevant clinical outcomes. In this dissertation, we studied three MRI methods for assessment of cerebral perfusion without exogenous contrast agents, quantification of blood-brain barrier disruption, and improved detection of infratentorial ischemic damage.

Methods

In Study I, we compared a contrast agent-free method for measuring perfusion, known as BOLD delay (from the blood-oxygenation-level-dependent signal), to the clinical reference standard, dynamic susceptibility contrast MRI (DSC-MRI) in 30 stroke patients within 24 hours of symptom onset. In Study II, we used dynamic contrast-enhanced MRI (DCE-MRI) to quantify blood-brain barrier (BBB) leakage in 54 stroke patients within 48 hours of symptom onset. In Study III, we compared the diagnostic performance of a stimulated echo acquisition mode (STEAM) diffusion weighted imaging (DWI) sequence to that of the clinical reference standard, an echo planar imaging (EPI) DWI sequence, in 57 patients with suspected infratentorial stroke.

Results

BOLD delay was closely related to DSC-MRI parameters that reflect both macrovascular delay and microvascular perfusion and was capable of distinguishing severe hypoperfusion from milder blood flow changes (Study I). We quantified BBB permeability and observed an increase in leakage over time in ischemic lesions. Leakage was also present in contralateral tissue, where it decreased over time (Study II). STEAM-DWI showed good agreement with EPI-DWI and a high sensitivity to ischemia, with far fewer intraparenchymal artifacts than EPI-DWI (Study III).

Conclusions

This dissertation shows that BOLD delay, DCE-MRI, and STEAM-DWI can be incorporated into routine MRI protocols for the assessment of stroke patients. They provide useful information regarding perfusion, BBB permeability, and infratentorial ischemic damage and have the potential to influence acute stroke diagnosis and management. The dissertation also highlights several weaknesses of these methods, opening up paths for further research and improvement.

1.2 Abstract (deutsch)

Einführung

Innovative Magnetresonanztomographie-Techniken (MRT) bergen das Potential klinische Therapieentscheidungen beim akuten Schlaganfall positiv beeinflussen zu können. Diese Techniken müssen jedoch zuerst in der klinischen Routine evaluiert und genau validiert werden, indem man sie mit etablierten Methoden und deren Ergebnissen vergleicht. In dieser Dissertation wurden drei MRT-Techniken zum verbesserten Nachweis infratentorieller Schlaganfälle, Beurteilung der Bluthirnschranken-Störung und Kontrastmittel-freien Perfusion untersucht.

Methoden

In Studie I wurde eine Kontrastmittel-freie Methode der Perfusionsmessung, bekannt als "BOLD („blood-oxygenation-level-dependent“) delay" mit dem klinischen Referenzstandard, der DSC-MRT („dynamic susceptibility contrast“) bei 30 Schlaganfallpatienten innerhalb von 24 Stunden nach Symptombeginn verglichen. In Studie II wurde die DCE-MRT („dynamic contrast-enhanced“) eingesetzt, um eine Störung der Bluthirnschranke bei 54 Schlaganfallpatienten innerhalb von 48 Stunden nach Symptombeginn quantitativ erfassen zu können. In Studie III wurde die diagnostische Aussagekraft der STEAM („stimulated echo acquisition mode“) diffusions-gewichtete (DWI) Sequenz mit der klinischen Referenzmethode, der echoplanaren (EPI=echo planar imaging) DWI bei 57 Patienten mit fraglichen infratentoriellen Schlaganfall evaluiert.

Ergebnisse

Die BOLD Technik zeigte einen engen Zusammenhang mit DSC-MRT Parametern hinsichtlich Folgen von Stenosen/Verschlüssen der zerebralen Arterien. Eine schwere Minderdurchblutung konnte von leichten Veränderungen der Blutflusses unterschieden werden (Studie I). Störungen der Bluthirnschranke konnten quantitativ erfaßt und eine weitere Zunahme im ischämischen Areal im zeitlichen Verlauf beobachtet werden. Eine Störung der Bluthirnschranke fand sich auch im „gesunden“ kontraläsionalen Hirngewebe, die sich im zeitlichen Verlauf besserte (Studie II). Die STEAM-DWI zeigte eine gute Übereinstimmung mit der EPI-DWI und eine hohe Sensitivität mit deutlich weniger intraparenchymalen Artefakten als die EPI-DWI (Studie III).

Schlußfolgerungen

Diese Dissertation konnte zeigen, daß der BOLD delay, die DCE-Technik und die STEAM-DWI für die MRT Schlaganfalldiagnostik in Routine-Protokolle inkorporiert werden könnte. Damit stünden aussagekräftige Zusatzinformationen zu Perfusion, Bluthirnschrankenpermeabilität und Detektion von infratentoriellen Schlaganfällen zur Verfügung mit der Möglichkeit besserer Therapieoptionen. Diese Dissertation zeigt auch die Schwächen dieser Methoden auf und eröffnet damit einen Weg für weitere Forschungsmöglichkeiten und Verbesserungen.

1.3 Introduction

When a patient presents with clinical features suggestive of acute stroke, the immediate aims are to confirm the diagnosis, to determine whether this particular patient is likely to benefit from or be harmed by treatment, and to treat them as fast as possible (when indicated). Medical imaging plays an important role in the first two of these aims as well as in monitoring the effects of treatment and the progression of stroke. Magnetic resonance imaging (MRI) is particularly useful for this purpose as it allows a lot of relevant information to be gathered. Although generally considered slower to acquire and analyze than computed tomography (CT), which has been the standard imaging modality used in acute stroke for decades, MRI does not need to be prohibitively time consuming. Several centers have implemented acute stroke MR protocols[1–3] within recommended hospital arrival-to-treatment times[4].

Such protocols include carefully selected sequences that assess pathophysiological processes that are relevant to stroke patients' management[5–7]. T2*-weighted sequences are used to exclude hemorrhage, and diffusion weighted imaging (DWI) sequences detect areas of severe ischemic cellular damage, including irreversible infarction. This is important for excluding stroke mimics, classifying stroke subtypes, and assessing the risk of treatment complications. Vessel stenosis or occlusion can be visualized using MR angiography, which also helps to classify stroke subtypes and plan mechanical thrombectomy. Fluid-attenuated inversion recovery (FLAIR) sequences are used to assess the age of ischemic lesions, including differentiating acute from chronic ischemic damage and estimating the time of stroke onset in patients without a clear known onset time. Perfusion imaging can help predict which patients will respond best to treatment by detecting the presence or absence of damaged yet potentially salvageable tissue.

Despite the advances made in recent years in stroke imaging, most patients are still excluded from treatment in the acute phase because decision-making is based on simplistic time-based models[8]. The cause of this is probably multifactorial, including limited access to, and experience with, advanced MRI techniques in most hospitals. However, by improving imaging methods we can better investigate phenomena that may enhance the efficacy of available stroke therapies (as well as the development of new therapeutic options) and the quality of decision-making itself (i.e., determining which criteria to use for treatment). This is especially relevant for patients who are currently left untreated with thrombolysis and thrombectomy but who may yet benefit if more information from advanced imaging helps guide the decision-making process. Ultimately, however, the usefulness of any imaging

technique in acute stroke involves a pragmatic compromise between diagnostic performance, the time taken to acquire the data, the complexity of the data acquisition and analysis, and the robustness of the method to patient-related factors[9].

The complex pathophysiology of acute stroke offers a plethora of opportunities for improving patient outcomes (Figure 1). Having appropriate tools for testing whether or not certain pathophysiological processes, and their modulation by therapy, are relevant to the management of acute stroke patients is critical. In this dissertation, the use of emerging MRI techniques for measuring three key aspects of stroke pathophysiology, outlined individually below, is investigated.

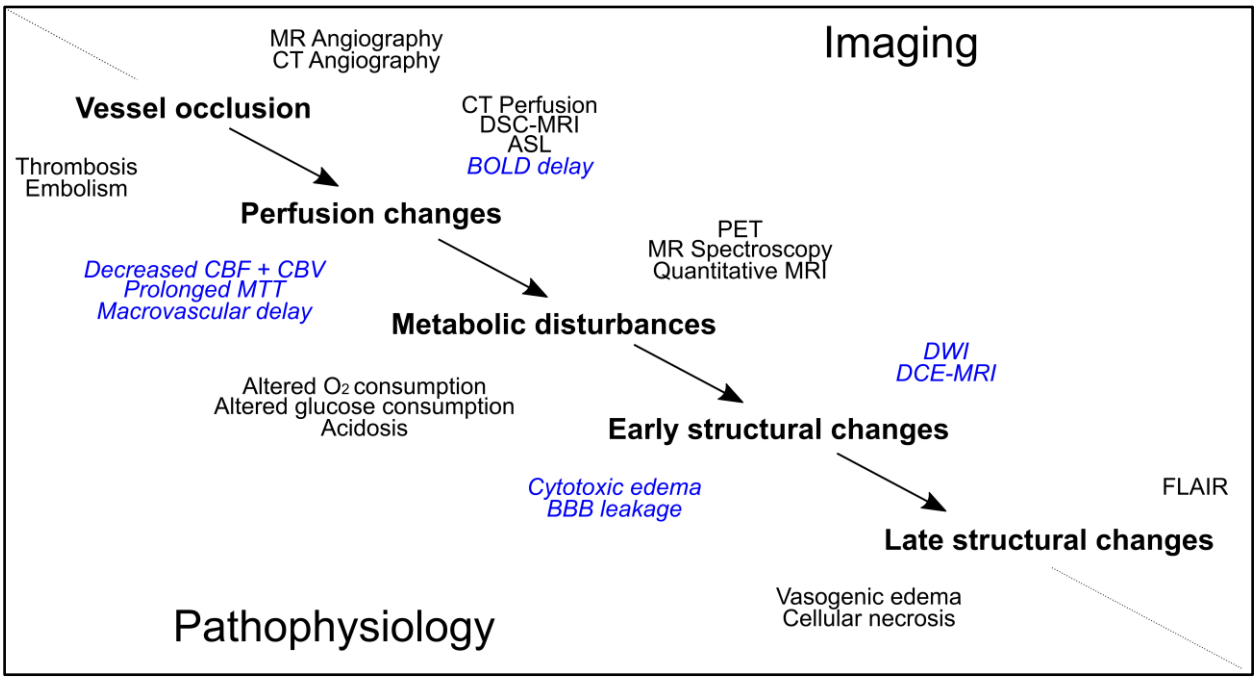

Figure 1— Overview of ischemic stroke pathophysiology, with a focus on processes measurable using clinically accessible medical imaging techniques in humans. Protective processes, such as the extent of collateral flow, also play a crucial role in stroke pathophysiology and can be assessed using medical imaging (not depicted here). The processes and methods primarily investigated in this dissertation are italicized and in blue. MR: magnetic resonance, CT: computed tomography, PET: positron emission tomography, CBF: cerebral blood flow, CBV: cerebral blood volume, MTT: mean transit time, BBB: blood-brain barrier, DSC: dynamic susceptibility contrast, ASL: arterial spin labelling, DWI: diffusion weighted imaging, DCE: dynamic contrast-enhanced, FLAIR: fluid-attenuated inversion recovery.

1.3.1 Cerebral perfusion

An immediate consequence of the occlusion of a brain artery is reduced blood flow to the area supplied by that vessel. Part of this area, the ischemic penumbra, is characterized by severely reduced blood flow and reversible cessation of normal electrical neural activity[10]. The penumbra represents the tissue at risk of being permanently damaged as time passes and its detection helps identify whom to treat, and therefore avoids potential side effects in patients with a low chance of responding favorably to reperfusion therapy. It also allows treatment of patients who would otherwise be excluded[11], such as those presenting beyond conventional time windows or without detectable infarction at presentation[12].

A number of approaches can be used to visualize the penumbra in clinical practice. Most commonly, perfusion is measured using dynamic susceptibility contrast MRI (DSC-MRI), where a paramagnetic contrast agent (usually gadolinium-based) is injected intravenously. The resulting signal loss on a rapidly acquired T2*-weighted sequence is used to infer information about blood flow[13]. This well-established technique is not without its limitations, most prominently the potential side effects of gadolinium. These include kidney damage[14] and long-term deposition in the brain, the consequences of which are yet to be fully understood[15]. The results of this technique are also highly dependent on how the data are acquired and processed[16–18], making reproducibility and standardization difficult.

A commonly used alternative that does not require an exogenous contrast agent is arterial spin labelling (ASL). Cerebral blood flow is calculated from the differences in brain tissue magnetization measured before and after inverting the magnetization ("labelling") of water protons in the neck arteries with radiofrequency pulses. ASL has certain drawbacks compared to DSC-MRI, including low SNR and an inherent sensitivity to head motion[19]. Crucially, its interpretation is difficult when the time it takes the labelled blood to travel from the labelling area to the measurement area is unknown. This occurs in patients with severe atherosclerotic disease affecting the large vessels[20], although attempts have recently been made to circumvent this problem[21].

The shortcomings of existing methods, and the fact that no single available method is likely to be appropriate for all patients, have motivated a search for novel non-invasive techniques to measure perfusion in stroke patients. This includes using the blood-oxygenation-level-dependent (BOLD) signal as an endogenous source of blood flow contrast[22]. In Study I of this dissertation, we quantitatively compared the results of a BOLD-based technique, known as BOLD delay, to that of the clinical reference standard for measuring perfusion, DSC-MRI, in acute ischemic stroke[23].

1.3.2 Blood-brain barrier permeability

The blood-brain barrier (BBB), the lining of brain capillaries by endothelial cells sealed by tight junctions, is disrupted in stroke, allowing the passage of large molecules into brain tissue. This increased permeability is associated with complications such as hemorrhagic transformation[24,25] and vasogenic edema[26]. Until recently, the evaluation of BBB permeability in acute stroke patients has been done either in a semi-quantitative manner, which is difficult to interpret and not as sensitive to subtle permeability changes[27], or with long acquisition times (up to 30 minutes)[28], making it difficult to implement in a routine clinical setting.

In Study II of this dissertation, we used an MRI approach with a short (six-minute) acquisition time to quantify BBB permeability in a group of stroke patients[29].

1.3.3 Cerebral ischemic cellular damage

Ischemic cellular damage (cytotoxic edema) is a consequence of the metabolic changes brought about by a severe reduction in blood flow. DWI has a very high sensitivity for detecting such ischemic changes[30]. However, ischemic damage is often mimicked or concealed on standard DWI sequences by anisotropic diffusion and magnetic susceptibility artifacts, respectively. This is particularly relevant in the infratentorial compartment, where ischemic lesions are often less conspicuous and small and where artifacts are prominent because of tissue-air interfaces near the skull base[31,32].

In Study III of this dissertation, we assessed the clinical utility of a DWI sequence that is less prone to susceptibility artifacts, known as stimulated echo acquisition mode DWI (STEAM-DWI), by directly comparing its diagnostic performance to conventional DWI methods (echo planar imaging DWI; EPI-DWI) in a group of stroke patients[33].

1.4 Objectives

This dissertation aimed to bridge technical innovations in MR methods with their practical application by validating three different MR techniques in the setting of acute ischemic stroke. This involved testing them as part of a routine clinical workflow and comparing them to more established methods. The eventual goal is to use these emerging methods in practice to better characterize acute stroke patients and help make more informed and justified clinical decisions.

The specific objectives of this dissertation were as follows:

- Study I (Publication 1): To compare hypoperfusion measured using a novel, non-invasive perfusion MRI technique (**BOLD delay**) with the current clinical reference standard, DSC-MRI[23].
- Study II (Publication 2): To quantify and monitor blood-brain barrier leakage in acute ischemic stroke using **DCE-MRI**[29].
- Study III (Publication 3): To assess the diagnostic performance of a DWI sequence that is less prone to artifacts (**STEAM-DWI**) compared to the clinical reference standard (EPI-DWI) for detecting infratentorial ischemic tissue damage[33].

1.5 Methods

This section provides a conceptual description of the main MRI techniques assessed in this dissertation. The specific methodologies of each study, including the study design, patient selection criteria, image processing, outcome measures, and statistical analysis, are described in detail in the attached original publications.

All data were derived from two prospective, observational clinical studies (the 1000plus study[2], *clinicaltrials.gov NCT00715533* and Longitudinal MRI Examinations of Patients With Brain Ischemia and Blood-Brain Barrier Permeability [LOBI-BBB], *clinicaltrials.gov NCT02077582*) that were approved by the ethics committee of the Charité Universitätsmedizin Berlin. Patients gave written informed consent to participate. Imaging was performed on a 3T Siemens Tim Trio MRI scanner adjacent to the stroke unit of a large university hospital (Charité Campus Benjamin Franklin, Berlin). All sequences investigated in this dissertation were incorporated into a routine stroke imaging protocol[2].

1.5.1 Assessing cerebral perfusion without exogenous contrast agents

The effect of deoxyhemoglobin on R2* is the basis of the BOLD signal. Slow fluctuations in the BOLD signal at rest (known as *low frequency oscillations*; LFOs) reflect hemodynamic responses to neuronal activity (neurovascular coupling)[34] and other mechanisms that produce slow, oscillatory changes in cerebral blood flow. Although the former is what is typically sought after in resting-state functional connectivity experiments[35], the latter (referred to here as *vascular* LFOs) contributes a large deal to the total measured BOLD signal[36,37].

Of these, *local* vascular LFOs are a consequence of vessel wall motion, are modulated by changes in sympathetic nervous system activity and partially entrained by slow changes in neuronal activity[38]. *Systemic* vascular LFOs, on the other hand, originate from outside the brain but also contribute to the resting BOLD signal. Evidence for their extracerebral origin comes from the observation that cerebral BOLD signal oscillations correlate strongly with fluctuations in blood flow measured peripherally, for example recorded in the extremities using near-infrared spectroscopy[39]. A substantial component (~25%) of systemic LFOs originates from heart rate and blood pressure variations[40]. Importantly, systemic LFOs are physiological signals in and of themselves, and not the result of aliasing of higher-frequency signals when data are undersampled[41], nor are they directly related to neurovascular coupling[42]. They oscillate at the same frequencies as neuronal and local vascular LFOs and cause changes in R2* that are similar to those caused by neurovascular coupling, unlike the much faster BOLD signal changes caused by cyclical cardiac and respiratory activity[37]. Their spatial and temporal distribution closely resembles cerebral blood flow, travelling from the arteries through the gray matter to the veins in about 6 seconds, similar to the time it takes for blood to pass through the brain[43].

Because LFOs in the BOLD signal partially reflect travelling waves originating from outside the brain, tracking their path can be used to assess tissue perfusion. Time shift analysis (Figure 2) involves cross-correlating the BOLD signal time course of each voxel in the brain with a reference time course (both filtered to retain only the low frequencies)[22,44]. The reference can be the average signal from the entire brain[23,45–47], the healthy hemisphere[22,46], the major venous sinuses[23,45], or a recursively-generated signal[42,48]. The time shift that corresponds to the maximum correlation coefficient is identified, and used as a measure of how delayed the voxel's LFOs are compared to the reference signal's LFOs. Voxelwise maps generated using this procedure are referred to as time shift analysis or BOLD delay maps.

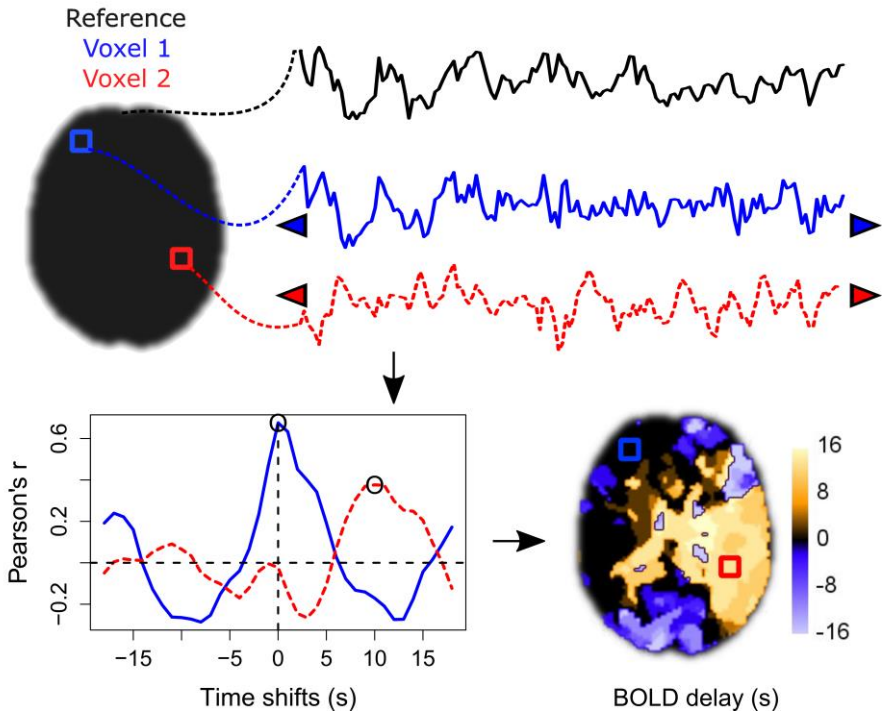

Figure 2 – Schematic of time shift analysis. The BOLD signal time course of a voxel (shown here for two voxels – 1 & 2) is time-shifted (arrowheads) and correlated at each time shift with the reference time course (in this case, the average BOLD signal across the entire brain). A plot of the correlation coefficient (Pearson's r) at each time shift shows how the time shift step corresponding to the maximum correlation between the two signals is identified (black circles) and represents the BOLD delay value. Note that the extent to which the signals are shifted (the limits of the x-axis on the plot) is known as the time shift range. The result of doing this for all voxels in the brain is a BOLD delay map, where areas of low perfusion have positive BOLD delay values (voxel 2) and areas of normal perfusion have a BOLD delay of zero (voxel 1). Adapted in part from Lv et al., Ann. Neurol. 2013.

In Study I, thirty patients with supratentorial stroke received DSC-MRI and resting-state functional MRI within 24 hours of symptom onset. Patients with severe head motion (a spike of >3 mm or a mean framewise displacement of >0.5 mm in the resting-state scan) were excluded. Values of BOLD delay (calculated using both a whole-brain and venous sinus reference, using three time shift ranges) and the coefficient of variation of the BOLD signal were compared to four DSC-MRI parameters in 156 regions of interest using Pearson correlation coefficient and multiple linear regression. In addition, a receiver operating characteristic (ROC) analysis assessed the performance of each measure for detecting the presence of severely hypoperfused tissue (defined as Tmax delay > 6 s).

1.5.2 Quantifying blood-brain barrier leakage

Low-molecular weight paramagnetic contrast agents, such as gadolinium, extravasate into the extracellular space when the blood-brain barrier is disrupted. They prolong the longitudinal relaxation rate (R1), causing a hyperintense signal on post-contrast T1-weighted images. In dynamic contrast-enhanced MRI (DCE-MRI), multiple T1-weighted images are acquired after contrast agent injection. The relationship between the change in signal intensity over time and contrast agent concentration provides information about blood flow, blood volume, and the permeability of the microvasculature. One quantitative method for analyzing DCE-MRI data is the Patlak model, which considers two compartments (blood plasma and extracellular space) and is described by the following equation[49]:

$$C_t(t) = v_p C_p(t) + K^{Trans} \int_0^t C_p(\tau) d\tau$$

In this equation, t is the time after contrast agent injection, C_t is the contrast agent concentration in the tissue, K^{Trans} is the rate of contrast agent delivery to the extracellular space per volume of tissue (normalized to the arterial plasma concentration), C_p is the plasma contrast agent concentration, and v_p is the fractional plasma volume. Using linear regression, K^{Trans} and v_p can be obtained. The Patlak model assumes a lack of backflux of contrast agent from the extracellular space to the blood (unidirectional transport), a low rate of contrast agent extravasation, and sufficient blood flow. This model was found to be generally robust and particularly appropriate for situations where permeability is low, such as stroke[27].

Calculating the parameters in the Patlak equation requires mapping the longitudinal relaxation time (T1). In Study II, this was done using a 3D spoiled fast low angle shot (FLASH) sequence with multiple flip angles before contrast agent injection. This was followed by acquiring repeated single flip angle 3D FLASH images, starting one minute before a continuous infusion of 10 mL of gadobutrol. In total, 54 stroke patients within 48 hours of symptom onset (28 of whom had a follow-up 5–7 days later) were investigated. The skull, scalp, cerebrospinal fluid, and blood vessels were removed from the T1-weighted images. Each patient's DWI was registered to the corresponding T1-weighted image. K^{Trans} values within the acute DWI lesion and a contralateral region of interest were extracted for all patients and timepoints and compared using the Wilcoxon signed-rank test. Permeability changes over time, adjusted for potential confounders, were assessed using a linear mixed model.

1.5.3 Improved detection of cerebral ischemic cellular damage

The diffusion of water molecules can be measured using MRI and allows the visualization of cytotoxic edema, which is characterized by sequestration of water inside cells, where diffusion is limited by intracellular organelles. In diffusion-weighted imaging (DWI) sequences, a radiofrequency (RF) pulse is applied in the presence of a strong magnetic field ("diffusion-encoding") gradient. The phase shift acquired by a spin as a result depends on how strong the magnetic field (which includes the main magnetic field and the diffusion-encoding gradient) is at the spin's location. A "refocusing" RF pulse (180°) is then applied to invert this phase shift. Because stationary spins will experience the same local magnetic field before and after the refocusing pulse, their cumulative phase shifts will be zero and an echo signal with maximum amplitude will be formed. In contrast, a moving spin will be exposed to a different local magnetic field strength (due to its different position) and will acquire a phase shift that is proportional to the spin's displacement in the direction of the diffusion-encoding gradient. As a result, the cumulative phase shifts of moving spins will be non-zero, resulting in a reduction in the MR signal[50].

Conventional diffusion-weighted sequences use a 90° RF pulse followed by a 180° RF pulse, with diffusion gradients applied in between, to generate a spin echo[50]. They typically combine this with an echo planar imaging (EPI) readout, acquiring multiple lines of k-space (effectively sampling all data points needed to reconstruct an image) within a single shot. This greatly shortens acquisition time but renders the sequence vulnerable to artifacts such as susceptibility-related signal losses and chemical shift effects[50].

Diffusion-weighted stimulated echo acquisition mode (STEAM) sequences combine a series of at least three RF pulses, that collectively induce what is known as a stimulated echo (STE), with diffusion-encoding gradients (Figure 3)[51]. The interval between the second and third pulses (the mixing time) largely determines the diffusion weighting. During this time, spins experience only T1 (longitudinal) relaxation, which is much longer than the T2 (transverse) relaxation that occurs in the first and third intervals. Signal decay is therefore slower in a STEAM sequence, allowing long mixing times to be used. Due to the flip angles of the applied RF pulses and the partial T1 relaxation occurring during the mixing time, the maximum magnitude of a STE is only half that of a spin echo[50,52]. However, compared to conventional DWI, the technique has the advantage of being far less prone to susceptibility-related signal losses, even with single-shot acquisitions[51].

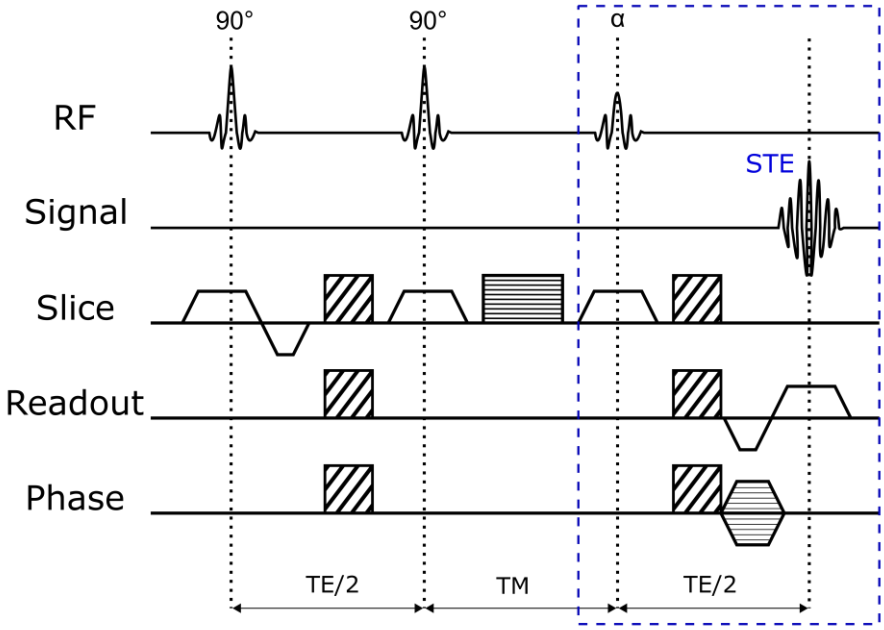

Figure 3 – Schematic diagram of a diffusion imaging pulse sequence using stimulated echoes (STE). Diffusion-encoding gradients (diagonal stripes) are placed within the first and third intervals – the summed duration of these two intervals is the echo time (TE). The crusher gradient (horizontal stripes) during the mixing time (TM) dephases the transverse magnetization, eliminating any spin echoes generated by the first two 90° RF pulses. For high-speed (single-shot) imaging, the part within the dashed box can be repeated using a succession of slice-selective low flip angle excitation pulses (α) and varying phase encoding gradient values. Adapted from Merboldt et al., Magn. Reson. Med. 1992.

In Study III, we calculated inter-modality and inter-rater agreement for STEAM-DWI and two EPI-DWI sequences (with different slice thicknesses – 5 mm [LR-DWI] or 2.5 mm [HR-DWI]) in 57 patients with suspected infratentorial stroke and no contraindication to MRI consecutively recruited between March 2010 and October 2011. Each patient's images (all 3 DWI sequences) were checked for the presence of ischemic lesions and intraparenchymal artifacts by two raters (one senior and one junior). Cohen's kappa, overall raw agreement, proportions of specific agreement, and the intraclass correlation coefficient were calculated for the presence of ischemic lesions. We also calculated the sensitivity of each sequence to infratentorial ischemia in a subset of 45 patients with a final diagnosis of infratentorial infarction, confirmed by persistence of the neurological deficit and/or follow-up MRI showing the final infarct.

1.6 Results

1.6.1 Assessing cerebral perfusion without exogenous contrast agents

The following shows the relationship between the DSC-MRI perfusion parameters (time-to-maximum [Tmax], mean transit time [MTT], cerebral blood flow [CBF], and cerebral blood volume [CBV]) and the BOLD-based perfusion parameters. For the latter, "WB" and "VS" refer to the reference signal used for time shift analysis (whole-brain and venous sinus respectively), and the numbers (3, 7, or 10) are the time shift ranges – the number of time shifts (in units of repetition time) performed for finding the maximum correlation coefficient. "CoV" is the coefficient of variation of the BOLD signal.

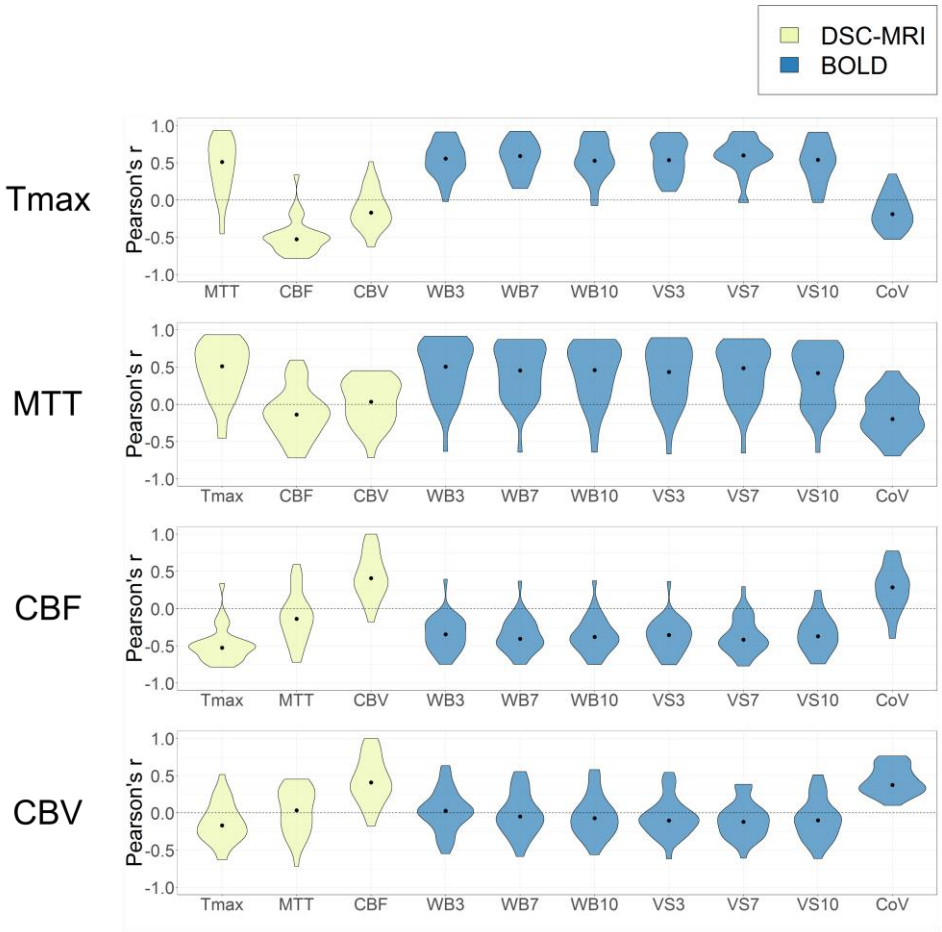

Figure 4 – The relationship between each DSC-MRI perfusion parameter and the rest of the parameters. Violin plots showing the distribution in the study sample of Pearson correlation coefficients (calculated for each individual patient, n = 30) between perfusion parameter values extracted from a custom atlas composed of 156 regions of interest (for details, see Supplemental Material in Khalil et al., Stroke 2017). Black dots show the median in the study sample.

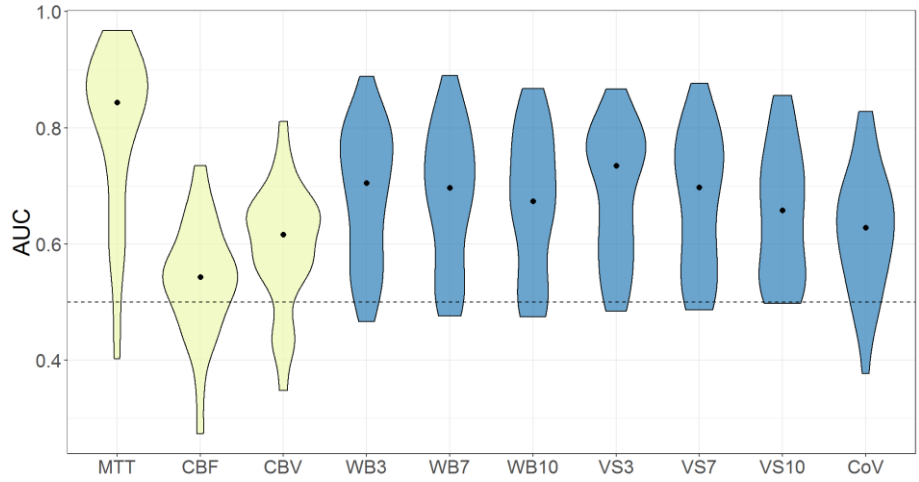

Figure 5 – Violin plots showing the distribution of area under the curve (AUC) values for each of the perfusion parameters (calculated for each individual patient, n = 30) for identifying severe hypoperfusion, defined as a Tmax delay of > 6 seconds. Black dots show the median in the study sample and the dashed line corresponds to an AUC of 0.5, suggestive of random prediction.

1.6.2 Quantifying blood-brain barrier leakage

The 54 stroke patients in our sample were scanned at baseline a median of 35 hours following symptom onset (interquartile range [IQR] = 25 – 41 hours) and had a median NIHSS of 4 at admission (IQR = 2 – 8). MR angiography showed vessel occlusion and stenosis in 37.0% and 20.4% of the patients, respectively.

We observed a median K^{Trans} of 0.7 (IQR = 0.4 – 1.8) × 10^{-3} min^{-1} in the DWI lesion, compared to 0.2 (IQR = 0.1 – 0.7) × 10^{-3} min^{-1} in the contralateral tissue (Wilcoxon signed-rank test, $p < 0.001$). Hemorrhagically transformed ischemic tissue had a higher median K^{Trans} of 1.8 (n = 11, IQR = 1.2 – 2.2) × 10^{-3} min^{-1} than the DWI lesions without hemorrhagic transformation (n = 43, median K^{Trans} = 0.7 × 10^{-3} min^{-1}, IQR = 0.4 – 2.0 × 10^{-3} min^{-1}, Wilcoxon signed-rank test, $p = 0.055$).

In the 28 patients who received follow-up imaging, median K^{Trans} values in the DWI lesion increased from 1.1 (IQR = 0.5 – 1.9) × 10^{-3} min^{-1} to 2.3 (IQR = 0.8 – 4.6) × 10^{-3} min^{-1} within the first week (linear mixed model, $p < 0.001$). This increase was most prominent in patients with baseline vessel occlusion or stenosis (linear mixed model, $p = 0.046$). K^{Trans} decreased from a median of 0.3 (IQR = 0.1 – 0.8) × 10^{-3} min^{-1} to 0.1 (IQR = 0.0 – 0.6) × 10^{-3} min^{-1} in the contralateral tissue within the first week (linear mixed model, $p = 0.052$).

1.6.3 Improved detection of cerebral ischemic cellular damage

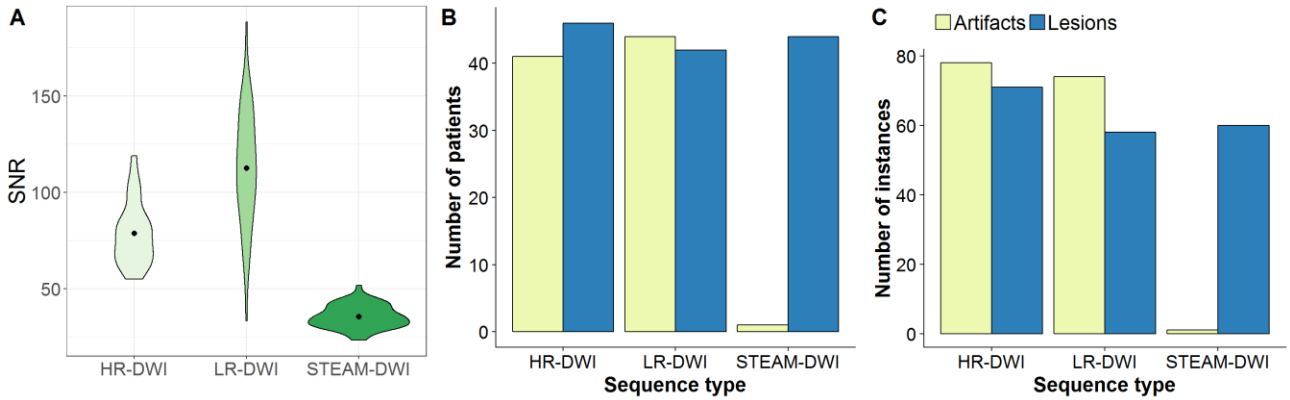

Figure 6 – A) Violin plots showing the distributions of signal-to-noise ratios (SNR) of the DWI sequences in the study sample. Black dots indicate the mean. B) Bar plot showing the number of patients in the study sample (total n = 57) with at least one ischemic lesion or artifact for each DWI sequence. C) Bar plot showing the total number of ischemic lesions or artifacts in the study cohort for each DWI sequence. LR-DWI: low-resolution echo planar imaging DWI (5 mm slice thickness), HR-DWI: high-resolution echo planar imaging DWI (2.5 mm slice thickness), STEAM-DWI: Stimulated echo acquisition mode DWI.

Table 1 – Agreement of LR-DWI and STEAM-DWI with the HR-DWI reference standard on the presence of ischemic lesions (n = 57), based on the senior raters' judgement.

Sequence	kappa	Positive percent agreement (%)	Negative percent agreement (%)	Intraclass correlation coefficient (95% CI)
LR-DWI	0.80	95.5	84.6	0.77 (0.62 – 0.86)
STEAM-DWI	0.68	93.3	75.0	0.63 (0.45 – 0.76)

Inter-rater agreement (Cohen's kappa) on the presence of ischemic lesions was 0.55 ($p<0.0001$) for HR-DWI, 0.67 ($p<0.0001$) for LR-DWI, and 0.62 ($p<0.0001$) for STEAM-DWI.

Table 2 – The sensitivity of each DWI sequence to ischemia, calculated from the 45 patients (out of 57) where a definite final diagnosis of infratentorial stroke could be made.

Sequence	Number of positive scans	Sensitivity in % (95% CI)
HR-DWI	42	93.0 (81.7 – 98.6)
LR-DWI	39	87.0 (73.2 – 95.0)
STEAM-DWI	40	89.0 (76.0 – 96.3)

1.7 Discussion

This dissertation assessed the use of three MR imaging techniques for assessing blood flow, measuring blood-brain-barrier leakage, and detecting infratentorial cerebral ischemia in stroke patients. The results show that each of these techniques possesses substantial potential for being routinely used in stroke patients, both in terms of practicality and diagnostic performance. Crucially, the dissertation also identifies several points of potential improvement that are the focus of ongoing work.

1.7.1 Assessing cerebral perfusion without exogenous contrast agents

Although several prior studies had shown the feasibility of using BOLD delay to measure perfusion[22,45,47,53], our study provided the first comprehensive investigation of the relationship between blood flow and delayed BOLD signal oscillations. Within a clinically relevant time window of 24 hours following symptom onset, BOLD delay is closely and independently related to DSC-MRI perfusion parameters that reflect both macrovascular delay (time-to-maximum; Tmax) and microvascular perfusion (mean transit time; MTT). BOLD delay thresholds are also capable of detecting severely hypoperfused tissue, which is important for identifying tissue at risk of infarction[54].

Besides allowing assessment of functional connectivity, a single resting-state functional MRI scan can be used to assess changes in blood flow in more than one way. These include temporal delays as well as changes in the amplitude and frequency of LFOs[55–57]. For example, our study showed that the standard deviation of the BOLD signal closely reflects blood volume in stroke patients. The ability of the BOLD signal to provide many different types of information poses both an opportunity, that of measuring several relevant pathophysiological processes with a single scan, and a challenge, that of unravelling these processes. This necessitates investigating these processes in animal models[58] and using sophisticated statistical methods for decomposing complex signals, such as independent component analysis[59].

Our study also provides some insight into the feasibility of BOLD delay in routine clinical practice. Out of the 50 patients who were eligible for the study, 15 had to be excluded based on motion thresholds derived from functional connectivity studies (and a further 4 due to poor-quality DSC-MRI data), highlighting that motion is currently an important drawback of using BOLD delay in such populations. We are currently studying the effect of motion on BOLD delay empirically, and exploring the use of motion correction techniques to improve data quality.

The BOLD delay method is undergoing several other important improvements. We recently started applying it to ultra-fast multiband EPI sequences[60]. Preliminary evidence suggests that their high temporal resolution can separate LFOs from cyclical cardiac and respiratory activity that are otherwise aliased in sequences with long repetition times[61]. Multiband sequences can be also be used to shorten scan time while maintaining data quality[62]. We are also currently incorporating BOLD delay maps into the routine imaging workup of acute stroke patients in our hospital, which includes a workflow for calculating and visualizing the maps at the MR scanner immediately after acquiring the data.

1.7.2 Quantifying blood-brain barrier leakage

Previous studies assessing BBB leakage in acute stroke using DCE-MRI have been cross-sectional, involving relatively small samples or using long acquisition times[49]. In our study, we used a six-minute DCE-MRI protocol and found that BBB permeability was several times higher in stroke lesions than in contralateral tissue within the first 48 hours after symptom onset and increased further over time, particularly in patients with a vessel occlusion or stenosis at baseline. These findings have recently been independently replicated[25].

We also observed BBB dysfunction in apparently healthy tissue contralateral to the acute infarct. This was seen despite the thorough exclusion of blood vessels and cerebrospinal fluid, which may show high permeability values that contaminate nearby tissues through the partial volume effect. Widespread BBB leakiness exists in patients with microvascular dysfunction[63,64], a comorbidity commonly seen in stroke patients. However, we observed that this leakiness decreases upon follow-up imaging about a week after stroke onset, suggesting that it may instead reflect a global BBB disruption related to post-stroke neuroinflammation.

The clinical significance of BBB dysfunction and its trajectory over time in stroke patients is not yet well understood. Evidence suggests that BBB leakiness is associated with poor outcomes after stroke treatment[65] and its peak coincides with the development of hemorrhagic transformation and vasogenic edema[25,26]. The timing of this peak varies between patients[25], necessitating measurement on an individual basis, and emphasizing the need for a convenient and accurate method of doing so. Our group is currently acquiring more longitudinal data from acute stroke patients using DCE-MRI to better characterize the progression of BBB leakage over time and determine its clinical consequences.

Particularly in mild strokes, BBB leakage can be subtle. Its detection requires the use of both a sensitive acquisition technique and an appropriate pharmacokinetic model. Although the Patlak model

(used in Study II of this dissertation) is sensitive to subtle BBB dysfunction[27], an iterative data-driven model selection process may help determine the optimal method for analyzing a given dataset[66]. This approach has recently been applied in a study of three ischemic stroke patients[67] and can potentially improve the reliability of the calculated permeability metrics.

1.7.3 Improved detection of cerebral ischemic cellular damage

Although STEAM-DWI was used in some of the earliest work on detecting ischemic cellular damage using MRI in humans[68], its use eventually declined because EPI-DWI provided high-quality images with shorter scan times[69]. However, recent technical developments in STEAM-DWI, as well as the drawbacks of conventional (EPI-based) DWI in the infratentorial compartment, motivated us to explore its use for diagnosing brainstem and cerebellar stroke.

Our study emphasizes the fact that artifacts and ischemic lesions are easily mistaken for one another on conventional DWI. In many cases, the diagnosis of an infratentorial stroke cannot be made with confidence because of the presence of these artifacts. This results in infratentorial ischemic damage commonly being missed on routine imaging[70], with clinical consequences such as an inability to properly determine stroke etiology[32] or prevent post-stroke complications such as recurrence or disability[71]. In our study, STEAM-DWI showed similar diagnostic performance for detecting ischemic damage as routine DWI, with almost no relevant intraparenchymal artifacts.

STEAM-DWI generally takes longer to acquire and has a lower signal-to-noise ratio than EPI-DWI[33]. For this reason, STEAM-DWI is not recommended as a routine replacement for EPI-DWI in all cases. However, it may be useful when the diagnosis is in doubt, for example in patients with negative EPI-DWI but a clinical suspicion of an infratentorial stroke. It may also be useful for readers without extensive experience with stroke imaging (such as junior radiologists or neurologists), for whom the artifacts on conventional DWI may be particularly confusing. Since our study was published, substantial improvements have been made to the STEAM-DWI sequence that allow faster acquisitions with improved signal strength and image quality[72].

In conclusion, the three MR techniques investigated in this dissertation, none of which is currently routinely used in stroke imaging, are feasible in a clinical setting and provide valuable information about blood flow, BBB permeability, and tissue ischemia. Such techniques may help us investigate how these pathophysiological processes, and the interventions that potentially influence them, affect stroke patients' prognoses and clinical outcomes.

1.8 Bibliography

1. Shah S, Luby M, Poole K, Morella T, Keller E, Benson RT, Lynch JK, Nadareishvili Z, Hsia AW. Screening with MRI for Accurate and Rapid Stroke Treatment SMART. *Neurology*. 2015;84:2438–2444.

2. Hotter B, Pittl S, Ebinger M, Oepen G, Jegzentis K, Kudo K, Rozanski M, Schmidt WU, Brunecker P, Xu C, Martus P, Endres M, Jungehülsing GJ, Villringer A, Fiebach JB. Prospective study on the mismatch concept in acute stroke patients within the first 24 h after symptom onset - 1000Plus study. *BMC Neurol*. 2009;9:60.

3. Nael K, Khan R, Choudhary G, Meshksar A, Villablanca P, Tay J, Drake K, Coull BM, Kidwell CS. Six-Minute Magnetic Resonance Imaging Protocol for Evaluation of Acute Ischemic Stroke: Pushing the Boundaries. *Stroke*. 2014;45:1985–1991.

4. Fonarow GC, Smith EE, Saver JL, Reeves MJ, Hernandez AF, Peterson ED, Sacco RL, Schwamm LH. Improving door-to-needle times in acute ischemic stroke: The design and rationale for the American Heart Association/American Stroke Association's target: Stroke initiative. *Stroke*. 2011;42:2983–2989.

5. Wintermark M, Albers GW, Broderick JP, Demchuk AM, Fiebach JB, Fiehler J, Grotta JC, Houser G, Jovin TG, Lees KR, Lev MH, Liebeskind DS, Luby M, Muir KW, Parsons MW, Von Kummer R, Wardlaw JM, Wu O, Yoo AJ, Alexandrov A V., Alger JR, Aviv RI, Bammer R, Baron JC, Calamante F, Campbell BCV, Carpenter TC, Christensen S, Copen WA, Derdeyn CP, Haley EC, Khatri P, Kudo K, Lansberg MG, Latour LL, Lee TY, Leigh R, Lin W, Lyden P, Mair G, Menon BK, Michel P, Mikulik R, Nogueira RG, Ostergaard L, Pedraza S, Riedel CH, Rowley HA, Sanelli PC, Sasaki M, Saver JL, Schaefer PW, Schellinger PD, Tsivgoulis G, Wechsler LR, White PM, Zaharchuk G, Zaidat OO, Davis SM, Donnan GA, Furlan AJ, Hacke W, Kang DW, Kidwell C, Thijs VN, Thomalla G, Warach SJ. Acute stroke imaging research roadmap II. *Stroke*. 2013;44:2628–2639.

6. Warach SJ, Luby M, Albers GW, Bammer R, Bivard A, Campbell BC V, Derdeyn C, Heit JJ, Khatri P, Lansberg MG, Liebeskind DS, Majoie CBLM, Marks MP, Menon BK, Muir KW, Parsons MW, Vagal A, Yoo AJ, Alexandrov A V., Baron JC, Fiorella DJ, Furlan AJ, Puig J, Schellinger PD, Wintermark M. Acute Stroke Imaging Research Roadmap III Imaging Selection and Outcomes in Acute Stroke Reperfusion Clinical Trials: Consensus Recommendations and Further Research Priorities. *Stroke*. 2016;47:1389–1398.

7. Donahue MJ, Achten E, Cogswell PM, De Leeuw F-E, Derdeyn CP, Dijkhuizen RM, Fan AP, Ghaznawi R, Heit JJ, Ikram MA, Jezzard P, Jordan LC, Jouvent E, Knutsson L, Leigh R, Liebeskind DS, Lin W, Okell TW, Qureshi AI, Stagg CJ, van Osch MJ, van Zijl PC, Watchmaker JM, Wintermark M, Wu O, Zaharchuk G, Zhou J, Hendrikse J. Consensus statement on current and emerging methods for the diagnosis and evaluation of cerebrovascular disease. *J. Cereb. Blood Flow Metab.* 2017;0271678X1772183.

8. Demaerschalk BM, Kleindorfer DO, Adeoye OM, Demchuk AM, Fugate JE, Grotta JC, Khalessi AA, Levy EI, Palesch YY, Prabhakaran S, Saposnik G, Saver JL, Smith EE. Scientific Rationale for the Inclusion and Exclusion Criteria for Intravenous Alteplase in Acute Ischemic Stroke A Statement for Healthcare Professionals from the American Heart Association/American Stroke Association. *Stroke*. 2016;47:581–641.

9. Singer OC, Sitzer M, du Mesnil de Rochemont R, Neumann-Haefelin T. Practical limitations of acute stroke MRI due to patient-related problems. *Neurology*. 2004;62:1848–1849.

10. Leigh R, Knutsson L, Zhou J, van Zijl PC. Imaging the physiological evolution of the ischemic penumbra in acute ischemic stroke. *J. Cereb. Blood Flow Metab.* 2017;0271678X1770091.

11. Ryu WHA, Avery MB, Dharampal N, Allen IE, Hetts SW. Utility of perfusion imaging in acute stroke treatment: a systematic review and meta-analysis. *J. Neurointerv. Surg.* 2016;neurintsurg-2016-012751.

12. Hotter B, Ostwaldt AC, Levichev-Connolly A, Rozanski M, Audebert HJ, Fiebach JB. Natural course of total mismatch and predictors for tissue infarction. *Neurology*. 2015;85:770–775.

13. Villringer A, Rosen BR, Belliveau JW, Ackerman JL, Lauffer RB, Buxton RB, Chao Y -S, Wedeenand VJ, Brady TJ. Dynamic imaging with lanthanide chelates in normal brain: Contrast due to magnetic susceptibility effects. *Magn. Reson. Med.* 1988;6:164–174.

14. Khawaja AZ, Cassidy DB, Al Shakarchi J, McGrogan DG, Inston NG, Jones RG. Revisiting the risks of MRI with Gadolinium based contrast agents - review of literature and guidelines. *Insights Imaging*. 2015;6:553–558.

15. Gulani V, Calamante F, Shellock FG, Kanal E, Reeder SB. Gadolinium deposition in the brain: summary of evidence and recommendations. *Lancet Neurol.* 2017;16:564–570.

16. Schaafs L-A, Porter D, Audebert HJ, Fiebach JB, Villringer K. Optimising MR perfusion imaging: comparison of different software-based approaches in acute ischaemic stroke. *Eur. Radiol.* 2016;26:4204–4212.

17. Galinovic I, Ostwaldt AC, Soemmer C, Bros H, Hotter B, Brunecker P, Schmidt WU, Jungehülsing J, Fiebach JB. Search for a map and threshold in perfusion MRI to accurately predict tissue fate: A protocol for assessing lesion growth in patients with persistent vessel occlusion. *Cerebrovasc. Dis.* 2011;32:186–193.

18. Kane I, Carpenter T, Chappell F, Rivers C, Armitage P, Sandercock P, Wardlaw J. Comparison of 10 different magnetic resonance perfusion imaging processing methods in acute ischemic stroke: Effect on lesion size, proportion of patients with diffusion/perfusion mismatch, clinical scores, and radiologic outcomes. *Stroke*. 2007;38:3158–3164.

19. Donahue MJ, Juttukonda MR, Watchmaker JM. Noise concerns and post-processing procedures in cerebral blood flow (CBF) and cerebral blood volume (CBV) functional magnetic resonance imaging. *Neuroimage*. 2017;154:43–58.

20. Zaharchuk G. Arterial Spin Labeling for Acute Stroke: Practical Considerations. *Transl. Stroke Res.* 2012;3:228–235.

21. Martin SZ, Madai VI, von Samson-Himmelstjerna FC, Mutke MA, Bauer M, Herzig CX, Hetzer S, Günther M, Sobesky J. 3D GRASE Pulsed Arterial Spin Labeling at Multiple Inflow Times in Patients with Long Arterial Transit Times: Comparison with Dynamic Susceptibility-Weighted Contrast-Enhanced MRI at 3 Tesla. *J. Cereb. Blood Flow Metab.* 2015;35:392–401.

22. Lv Y, Margulies DS, Cameron Craddock R, Long X, Winter B, Gierhake D, Endres M, Villringer K, Fiebach J, Villringer A. Identifying the perfusion deficit in acute stroke with

resting-state functional magnetic resonance imaging. *Ann. Neurol.* 2013;73:136–139.

23. Khalil AA, Ostwaldt AC, Nierhaus T, Ganeshan R, Audebert HJ, Villringer K, Villringer A, Fiebach JB. Relationship between Changes in the Temporal Dynamics of the Blood-Oxygen-Level-Dependent Signal and Hypoperfusion in Acute Ischemic Stroke. *Stroke*. 2017;48:925–931.

24. Rosell A, Cuadrado E, Ortega-Aznar A, Hernández-Guillamon M, Lo EH, Montaner J. MMP-9-positive neutrophil infiltration is associated to blood-brain barrier breakdown and basal lamina type IV collagen degradation during hemorrhagic transformation after human ischemic stroke. *Stroke*. 2008;39:1121–1126.

25. Merali Z, Huang K, Mikulis D, Silver F, Kassner A. Evolution of blood-brain-barrier permeability after acute ischemic stroke. *PLoS One*. 2017;12:e0171558.

26. Neumann-Haefelin T, Kastrup A, De Crespigny A, Yenari MA, Ringer T, Sun GH, Moseley ME, Fisher M. Serial MRI After Transient Focal Cerebral Ischemia in Rats: Dynamics of Tissue Injury, Blood-Brain Barrier Damage, and Edema Formation. *Stroke*. 2000;31:1965–1973.

27. Heye AK, Thrippleton MJ, Armitage PA, Valdés Hernández M del C, Makin SD, Glatz A, Sakka E, Wardlaw JM. Tracer kinetic modelling for DCE-MRI quantification of subtle blood-brain barrier permeability. *Neuroimage*. 2016;125:446–455.

28. Wardlaw JM, Doubal F, Armitage P, Chappell F, Carpenter T, Muñoz Maniega S, Farrall A, Sudlow C, Dennis M, Dhillon B. Lacunar stroke is associated with diffuse Blood-Brain barrier dysfunction. *Ann. Neurol.* 2009;65:194–202.

29. Villringer K, Sanz Cuesta BE, Ostwaldt A-C, Grittner U, Brunecker P, Khalil AA, Schindler K, Eisenblätter O, Audebert H, Fiebach JB. DCE-MRI blood–brain barrier assessment in acute ischemic stroke. *Neurology*. 2017;88:433–440.

30. González RG, Schaefer PW, Buonanno FS, Schwamm LH, Budzik RF, Rordorf G, Wang B, Sorensen a G, Koroshetz WJ. Diffusion-weighted MR imaging: diagnostic accuracy in patients imaged within 6 hours of stroke symptom onset. *Radiology*. 1999;210:155–162.

31. Sylaja PN, Coutts SB, Krol A, Hill MD, Demchuk AM. When to expect negative diffusion-weighted images in stroke and transient ischemic attack. *Stroke*. 2008;39:1898–1900.

32. Engelter ST, Wetzel SG, Radue EW, Rausch M, Steck AJ, Lyrer PA. The clinical significance of diffusion-weighted MR imaging in infratentorial strokes. *Neurology*. 2004;62:574–80.

33. Khalil AA, Hohenhaus M, Kunze C, Schmidt W, Brunecker P, Villringer K, Merboldt KD, Frahm J, Fiebach JB. Sensitivity of diffusion-weighted STEAM MRI and EPI-DWI to infratentorial ischemic stroke. *PLoS One*. 2016;11:e0161416.

34. Ma Y, Shaik MA, Kozberg MG, Kim SH, Portes JP, Timerman D, Hillman EMC. Resting-state hemodynamics are spatiotemporally coupled to synchronized and symmetric neural activity in excitatory neurons. *Proc. Natl. Acad. Sci.* 2016;113:E8463–E8471.

35. Raichle ME, MacLeod AM, Snyder AZ, Powers WJ, Gusnard DA, Shulman GL. A default mode of brain function. *Proc. Natl. Acad. Sci. U. S. A.* 2001;98:676–82.

36. Tong Y, Hocke LM, Fan X, Janes AC, Frederick B deB. Can apparent resting state connectivity arise from systemic fluctuations? *Front. Hum. Neurosci.* 2015;9:285.

37. Liu TT. Noise contributions to the fMRI signal: An overview. *Neuroimage*. 2016;143:141–151.

38. Mateo C, Knutsen PM, Tsai PS, Shih AY, Kleinfeld D. Entrainment of Arteriole Vasomotor Fluctuations by Neural Activity Is a Basis of Blood-Oxygenation-Level-Dependent "Resting-State" Connectivity. *Neuron*. 2017;0.

39. Tong Y, Frederick B deB. Time lag dependent multimodal processing of concurrent fMRI and near-infrared spectroscopy (NIRS) data suggests a global circulatory origin for low-frequency oscillation signals in human brain. *Neuroimage*. 2010;53:553–564.

40. Katura T, Tanaka N, Obata A, Sato H, Maki A. Quantitative evaluation of interrelations between spontaneous low-frequency oscillations in cerebral hemodynamics and systemic cardiovascular dynamics. *Neuroimage*. 2006;31:1592–1600.

41. Tong Y, Hocke LM, Licata SC, Frederick B deB. Low-frequency oscillations measured in the periphery with near-infrared spectroscopy are strongly correlated with blood oxygen level-dependent functional magnetic resonance imaging signals. *J. Biomed. Opt.* 2012;17:106004.

42. Aso T, Jiang G, Urayama SI, Fukuyama H. A resilient, non-neuronal source of the spatiotemporal lag structure detected by bold signal-based blood flow tracking. *Front. Neurosci.* 2017;11:256.

43. Crandell D, Moinuddin M, Fields M, Friedman BI, Robertson J. Cerebral transit time of 99m technetium sodium pertechnetate before and after cerebral arteriography. *J. Neurosurg.* 1973;38:545–7.

44. Lv Y. Application of resting-state fMRI methods to acute ischemic stroke Dissertation. 2013;

45. Christen T, Jahanian H, Ni WW, Qiu D, Moseley ME, Zaharchuk G. Noncontrast mapping of arterial delay and functional connectivity using resting-state functional MRI: A study in moyamoya patients. *J. Magn. Reson. Imaging*. 2015;41:424–430.

46. Ni L, Li J, Li W, Zhou F, Wang F, Schwarz CG, Liu R, Zhao H, Wu W, Zhang X, Li M, Yu H, Zhu B, Villringer A, Zang Y, Zhang B, Lv Y, Xu Y. The value of resting-state functional MRI in subacute ischemic stroke: Comparison with dynamic susceptibility contrast-enhanced perfusion MRI. *Sci. Rep.* 2017;7:41586.

47. Siegel JS, Snyder AZ, Ramsey L, Shulman GL, Corbetta M. The effects of hemodynamic lag on functional connectivity and behavior after stroke. *J. Cereb. Blood Flow Metab.* 2016;36:2162–2176.

48. Tong Y, Frederick B de B. Tracking cerebral blood flow in BOLD fMRI using recursively generated regressors. *Hum. Brain Mapp.* 2014;35:5471–5485.

49. Heye AK, Culling RD, Valdés Hernández MDC, Thrippleton MJ, Wardlaw JM. Assessment of blood-brain barrier disruption using dynamic contrast-enhanced MRI. A systematic review. *NeuroImage Clin.* 2014;6:262–274.

50. Bammer R. Basic principles of diffusion-weighted imaging. *Eur. J. Radiol.* 2003;45:169–184.

51. Merboldt K-D, Hänicke W, Bruhn H, Gyngell ML, Frahm J. Diffusion Imaging of the Human Brain in Vivo Using High-Speed STEAM MRI. *Magn. Reson. Med.* 1992;192:179–192.

52. Burstein D. Stimulated echoes: Description, applications, practical hints. *Concepts Magn. Reson.* 1996;8:269–278.

53. Amemiya S, Kunimatsu A, Saito N, Ohtomo K. Cerebral Hemodynamic Impairment: Assessment with Resting-State Functional MR Imaging. *Radiology*. 2014;270:548–555.

54. Olivot JM, Mlynash M, Thijs VN, Kemp S, Lansberg MG, Wechsler L, Bammer R, Marks MP, Albers GW. Optimal tmax threshold for predicting penumbral tissue in acute stroke. *Stroke*. 2009;40:469–475.

55. Wang HH, Menezes NM, Ming WZ, Ay H, Koroshetz WJ, Aronen HJ, Karonen JO, Liu Y, Nuutinen J, Wald LL, Sorensen AG. Physiological noise in MR images: An indicator of the tissue response to ischemia? *J. Magn. Reson. Imaging*. 2008;27:866–871.

56. Tsai Y-H, Yuan R, Huang Y-C, Weng H-H, Yeh M-Y, Lin C-P, Biswal BB. Altered resting-state FMRI signals in acute stroke patients with ischemic penumbra. *PLoS One*. 2014;9:e105117.

57. Liu Y, D'Arceuil H, He J, Duggan M, Gonzalez G, Pryor J, De Crespigny A. MRI of spontaneous fluctuations after acute cerebral ischemia in nonhuman primates. *J. Magn. Reson. Imaging*. 2007;26:1112–1116.

58. Khalil AA, Mueller S, Foddis M, Dirnagl U, Fiebach JB, Villringer A, Boehm-Sturm P. Non-invasive assessment of cerebral perfusion using resting-state functional MRI in a mouse model of focal cerebral ischemia: preliminary results. In: European Molecular Imaging Meeting. Cologne: 2017.

59. Khalil A, Kirilina E, Nierhaus T, Villringer K, Villringer A, Fiebach J. Independent component analysis of resting-state hemodynamics in acute stroke: A new approach for identifying hypoperfusion. In: ESMRMB Congress. Vienna: 2016.

60. Xu J, Moeller S, Auerbach EJ, Strupp J, Smith SM, Feinberg DA, Yacoub E, Uğurbil K. Evaluation of slice accelerations using multiband echo planar imaging at 3T. *Neuroimage*. 2013;83:991–1001.

61. Khalil AA, Kirilina E, Villringer K, Fiebach JB, Villringer A. Perfusion maps based on temporal blood-oxygen-level-dependent signal delays are driven by alterations in low frequency oscillations between 0.01 and 0.1 Hz. In: JCBFM (BRAIN Conference). Berlin: SAGE Publications; 2017.

62. Khalil AA, Kirilina E, Villringer K, Villringer A, Fiebach JB. The Effect of Scan Length on the Assessment of Cerebral Perfusion Using Resting-state Functional MRI: A Comparison Between Sequences in Acute Stroke. In: ASNR 55th Annual Meeting. Long Beach, CA: 2017.

63. Topakian R, Barrick TR, Howe FA, Markus HS. Blood-brain barrier permeability is increased in normal-appearing white matter in patients with lacunar stroke and leucoaraiosis. *J. Neurol. Neurosurg. Psychiatry*. 2010;81:192–197.

64. Li Y, Li M, Zhang X, Shi Q, Yang S, Fan H, Qin W, Yang L, Yuan J, Jiang T, Hu W. Higher

blood–brain barrier permeability is associated with higher white matter hyperintensities burden. *J. Neurol.* 2017;264:1474–1481.

65. Leigh R, Christensen S, Campbell BCV, Marks MP, Albers GW, Lansberg MG. Pretreatment blood-brain barrier disruption and post-endovascular intracranial hemorrhage. *Neurology*. 2016;87:263–269.

66. Ewing JR, Bagher-Ebadian H. Model selection in measures of vascular parameters using dynamic contrast-enhanced MRI: Experimental and clinical applications. *NMR Biomed.* 2013;26:1028–1041.

67. Nadav G, Liberman G, Artzi M, Kiryati N, Bashat D Ben. Optimization of two-compartment-exchange-model analysis for dynamic contrast-enhanced mri incorporating bolus arrival time. *J. Magn. Reson. Imaging*. 2017;45:237–249.

68. Warach S, Chien D, Li W, Ronthal M, Edelman RR. Fast magnetic resonance diffusion-weighted imaging of acute human stroke. *Neurology*. 1992;42:1717–23.

69. Warach S, Gaa J, Siewert B, Wielopolski P, Edelman RR. Acute human stroke studied by whole brain echo planar diffusion-weighted magnetic resonance imaging. *Ann. Neurol.* 1995;37:231–241.

70. Chalela JA, Kidwell CS, Nentwich LM, Luby M, Butman JA, Demchuk AM, Hill MD, Patronas N, Latour L, Warach S. Magnetic resonance imaging and computed tomography in emergency assessment of patients with suspected acute stroke: a prospective comparison. *Lancet*. 2007;369:293–298.

71. Makin SDJ, Doubal FN, Dennis MS, Wardlaw JM. Clinically Confirmed Stroke With Negative Diffusion-Weighted Imaging Magnetic Resonance Imaging. *Stroke*. 2015;46:3142–3148.

72. Merrem A, Hofer S, Voit D, Merboldt K-D, Klosowski J, Untenberger M, Fleischhammer J, Frahm J. Rapid Diffusion-Weighted Magnetic Resonance Imaging of the Brain Without Susceptibility Artifacts. *Invest. Radiol.* 2017;52:428–433.

2 Affidavit

I, Ahmed Abdelrahim Ahmed Khalil, certify under penalty of perjury by my own signature that I have submitted the thesis on the topic "*Improved assessment of hypoperfusion, blood-brain barrier disruption, and ischemic cellular damage in stroke patients using magnetic resonance imaging*". I wrote this thesis independently and without assistance from third parties, I used no other aids than the listed sources and resources.

All points based literally or in spirit on publications or presentations of other authors are, as such, in proper citations (see "uniform requirements for manuscripts (URM)" the ICMJE www.icmje.org) indicated. The sections on methodology (in particular practical work, laboratory requirements, statistical processing) and results (in particular images, graphics and tables) correspond to the URM (s.o) and are answered by me. My contributions in the selected publications for this dissertation correspond to those that are specified in the following joint declaration with the responsible person and supervisor. All publications resulting from this thesis and which I am author of correspond to the URM (see above) and I am solely responsible.

The importance of this affidavit and the criminal consequences of a false affidavit (section 156,161 of the Criminal Code) are known to me and I understand the rights and responsibilities stated therein.

_____ _____

Date Signature

3 Declaration of contribution to the publications

Ahmed Abdelrahim Ahmed Khalil contributed as follows to these publications:

- Publication 1: **Khalil AA**, Ostwaldt AC, Nierhaus T, Ganeshan R, Audebert HJ, Villringer K, Villringer A, Fiebach JB. Relationship Between Changes in the Temporal Dynamics of the Blood-Oxygen-Level-Dependent Signal and Hypoperfusion in Acute Ischemic Stroke. Stroke. 2017 Apr 1;48(4):925-31.
    - Impact factor (2016) = **6.032**
    - Contribution in detail: Ahmed A Khalil conceived and designed this retrospective study, processed the rsfMRI and DSC-MRI data, and performed the statistical analysis and data visualization. He also interpreted the results, wrote all (first and subsequent) drafts of the manuscript and coordinated the journal submission process.
- Publication 2: Villringer K, Cuesta BE, Ostwaldt AC, Grittner U, Brunecker P, **Khalil AA**, Schindler K, Eisenblätter O, Audebert H, Fiebach JB. DCE-MRI blood–brain barrier assessment in acute ischemic stroke. Neurology. 2017 Jan 31;88(5):433-40.
    - Impact factor (2016) = **8.320**
    - Contribution in detail: Ahmed A Khalil contributed to the DCE-MRI data processing, including image registration and gray/white matter segmentation. He also contributed to the statistical analysis of the data and interpretation of the results and revised all drafts of the manuscript before submission.
- Publication 3: **Khalil AA**, Hohenhaus M, Kunze C, Schmidt W, Brunecker P, Villringer K, Merboldt KD, Frahm J, Fiebach JB. Sensitivity of diffusion-weighted STEAM MRI and EPI-DWI to infratentorial ischemic stroke. PloS one. 2016 Aug 16;11(8):e0161416.
    - Impact factor (2016) = **2.806**
    - Contribution in detail: Ahmed A Khalil contributed to the study design, statistically analyzed the rater data, performed the SNR/CNR analyses, and interpreted the results. He also visualized the imaging data, wrote all (first and subsequent) drafts of the manuscript and coordinated the journal submission process.

Signature, date, and stamp of the supervising university teacher

Signature of the doctoral candidate

_____ _____

4 Print versions of the selected publications

4.1 Publication 1

Khalil AA, Ostwaldt AC, Nierhaus T, Ganeshan R, Audebert HJ, Villringer K, Villringer A, Fiebach JB. Relationship between Changes in the Temporal Dynamics of the Blood-Oxygen-Level-Dependent Signal and Hypoperfusion in Acute Ischemic Stroke. *Stroke*. 2017;48:925–931.

https://doi.org/10.1161/STROKEAHA.116.015566

4.2 Publication 2

Villringer K, Cuesta BE, Ostwaldt AC, Grittner U, Brunecker P, **Khalil AA**, Schindler K, Eisenblätter O, Audebert H, Fiebach JB. DCE-MRI blood–brain barrier assessment in acute ischemic stroke. Neurology. 2017 Jan 31;88(5):433-440.

https://doi.org/10.1212/WNL.0000000000003566

4.3 Publication 3

Khalil AA, Hohenhaus M, Kunze C, Schmidt W, Brunecker P, Villringer K, Merboldt KD, Frahm J, Fiebach JB. Sensitivity of diffusion-weighted STEAM MRI and EPI-DWI to infratentorial ischemic stroke. *PLoS One*. 2016;11:e0161416.

PLOS ONE

RESEARCH ARTICLE

Sensitivity of Diffusion-Weighted STEAM MRI and EPI-DWI to Infratentorial Ischemic Stroke

Ahmed A. Khalil[1,2,3]*, Marc Hohenhaus[4], Claudia Kunze[1], Wolf Schmidt[1], Peter Brunecker[1], Kersten Villringer[1], Klaus-Dietmar Merboldt[5], Jens Frahm[5], Jochen B. Fiebach[1]

1 Center for Stroke Research Berlin, Charité – Universitätsmedizin Berlin, Berlin, Germany, **2** NeuroCure Cluster of Excellence, Charité – Universitätsmedizin Berlin, Berlin, Germany, **3** International Graduate Program Medical Neurosciences, Charité – Universitätsmedizin Berlin, Berlin, Germany, **4** Klinik für Neurochirurgie, Universitätsklinikum Freiburg, Freiburg im Breisgau, Germany, **5** Biomedizinische NMR Forschungs GmbH am Max-Planck-Institut für biophysikalische Chemie, Göttingen, Germany

* ahmed-abdelrahim.khalil@charite.de

Citation: Khalil AA, Hohenhaus M, Kunze C, Schmidt W, Brunecker P, Villringer K, et al. (2016) Sensitivity of Diffusion-Weighted STEAM MRI and EPI-DWI to Infratentorial Ischemic Stroke. PLoS ONE 11(8): e0161416. doi:10.1371/journal.pone.0161416

Editor: Terence J Quinn, University of Glasgow, UNITED KINGDOM

Received: May 29, 2016

Accepted: August 1, 2016

Published: August 16, 2016

Data Availability Statement: Data are from the 1000plus study whose authors may be contacted at jochen.fiebach@charite.de. Due to legal and ethical reasons, the MR images and clinical information are not publicly available. Single images will be provided by Ahmed Khalil (ahmed-abdelrahim.khalil@charite.de) upon request. All other data used in this study are publicly available from Figshare (DOIs 10.6084/m9.figshare.3495701 and 10.6084/m9.figshare.3496739).

Funding: This study received funding from the German Federal Ministry of Education and Research (https://www.bmbf.de/en/index.html) via the grant Center for Stroke Research Berlin (01EO0801 and

Abstract

Objectives

To assess the sensitivity of stimulated echo acquisition mode diffusion weighted imaging (STEAM-DWI) to ischemic stroke in comparison to echo-planar imaging diffusion weighted imaging (EPI-DWI) in the infratentorial compartment.

Methods

Fifty-seven patients presenting with clinical features of infratentorial stroke underwent STEAM-DWI, high-resolution EPI-DWI (HR-DWI, 2.5 mm slice thickness) and low-resolution EPI-DWI (LR-DWI, 5 mm slice thickness). Four readers assessed the presence of ischemic lesions and artifacts. Agreement between sequences and interobserver agreement on the presence of ischemia were calculated. The sensitivities of the DWI sequences were calculated in 45 patients with a confirmed diagnosis of infratentorial stroke.

Results

Median time from symptom onset to imaging was 24 hours. STEAM-DWI agreed with LR-DWI in 89.5% of cases (kappa = 0.72, p<0.0001) and with HR-DWI in 89.5% of cases (kappa = 0.68, p<0.0001). STEAM-DWI showed fewer intraparenchymal artifacts (1/57) than HR-DWI (44/57) and LR-DWI (41/57). Ischemia was visible in 87% of cases for LR-DWI, 93% of cases for HR-DWI, and 89% of cases for STEAM-DWI. Interobserver agreement was good for STEAM-DWI (kappa = 0.62, p<0.0001).

Conclusions

Compared to the best currently available MR sequence for detecting ischemia (HR-DWI), STEAM-DWI shows fewer artifacts and a similar sensitivity to infratentorial stroke.

01EO01301). The funders had no role in study design, data collection and analysis, decision to publish, or preparation of the manuscript.

Competing Interests: The authors have declared that no competing interests exist.

Introduction

Diffusion-weighted imaging (DWI) has a sensitivity exceeding 90% for detecting acute ischemia [1,2] and is routinely used for this purpose in clinical practice. However, commonly used DWI sequences, which combine a pulsed gradient spin-echo sequence and an echo-planar imaging (EPI) readout, show anisotropic diffusion and susceptibility artifacts. Such artifacts are particularly prominent in the infratentorial compartment and can hamper the detection of ischemic lesions in this area. The presence of these artifacts in the brainstem and cerebellum, where infarcts tend to be small and often inconspicuous, complicates the diagnosis of stroke using EPI-based DWI sequences [3–5].

DWI acquired with a slice-thickness of 2.5 mm is better at detecting ischemic lesions than that acquired with the more commonly used 5 mm slice thickness [6], most likely due to the higher spatial resolution. Therefore, despite taking longer to acquire and having a potentially lower signal-to-noise ratio, thin-slice DWI is considered the best available imaging tool in clinical practice for diagnosing cerebral ischemia. However, both these sequences are acquired with an EPI readout and therefore suffer from susceptibility artifacts. Diffusion-weighted images acquired using stimulated echo acquisition mode (STEAM-DWI) sequences are not affected by these artifacts [7–9], which makes them promising alternatives to conventional DWI sequences in infratentorial stroke. However, despite their potential advantages, the utility of STEAM-DWI sequences for diagnosing ischemic stroke has not yet been assessed.

In this study, we assessed the sensitivity to ischemia and the presence of intraparenchymal artifacts in three different DWI protocols (two EPI protocols with differing slice-thicknesses and one STEAM sequence). We hypothesized that STEAM-DWI would show fewer artifacts than both DWI protocols acquired using thin (2.5 mm) and thick (5 mm) slices and that the sensitivity of STEAM-DWI for detecting ischemia would be similar to conventional EPI-based DWI sequences.

Materials and Methods

Study design

This was a retrospective analysis of a prospective, single-center observational study (the 1000Plus study, ClinicalTrials.gov Identifier NCT00715533, full study protocol available here [10]), which received approval from the local ethics committee (Charité Ethikkommission, Ethikausschuss 4 am Campus Benjamin Franklin, Charitéplatz 1, 10177 Berlin; Institutional Review Board number EA4/026/08). All patients gave written informed consent.

Participants

Patients presenting to the emergency department who were clinically suspected of having an infratentorial stroke and who had no contraindications to MRI, were consecutively recruited between March 2010 and October 2011 at the Charité Campus Benjamin Franklin hospital in Berlin, Germany. Fig 1 shows a flowchart of the participants in this study.

Test methods

MR images were acquired on a Siemens Tim Trio 3T scanner with a 12-channel head coil.

All patients received a thick-slice DWI sequence (referred to henceforth as low-resolution DWI, LR-DWI), a thin-slice DWI sequence (referred to henceforth as high-resolution DWI, HR-DWI), and a STEAM-DWI sequence in addition to a standard stroke imaging protocol, the details of which have been published by Hotter et al. [10]. All three DWI sequences were

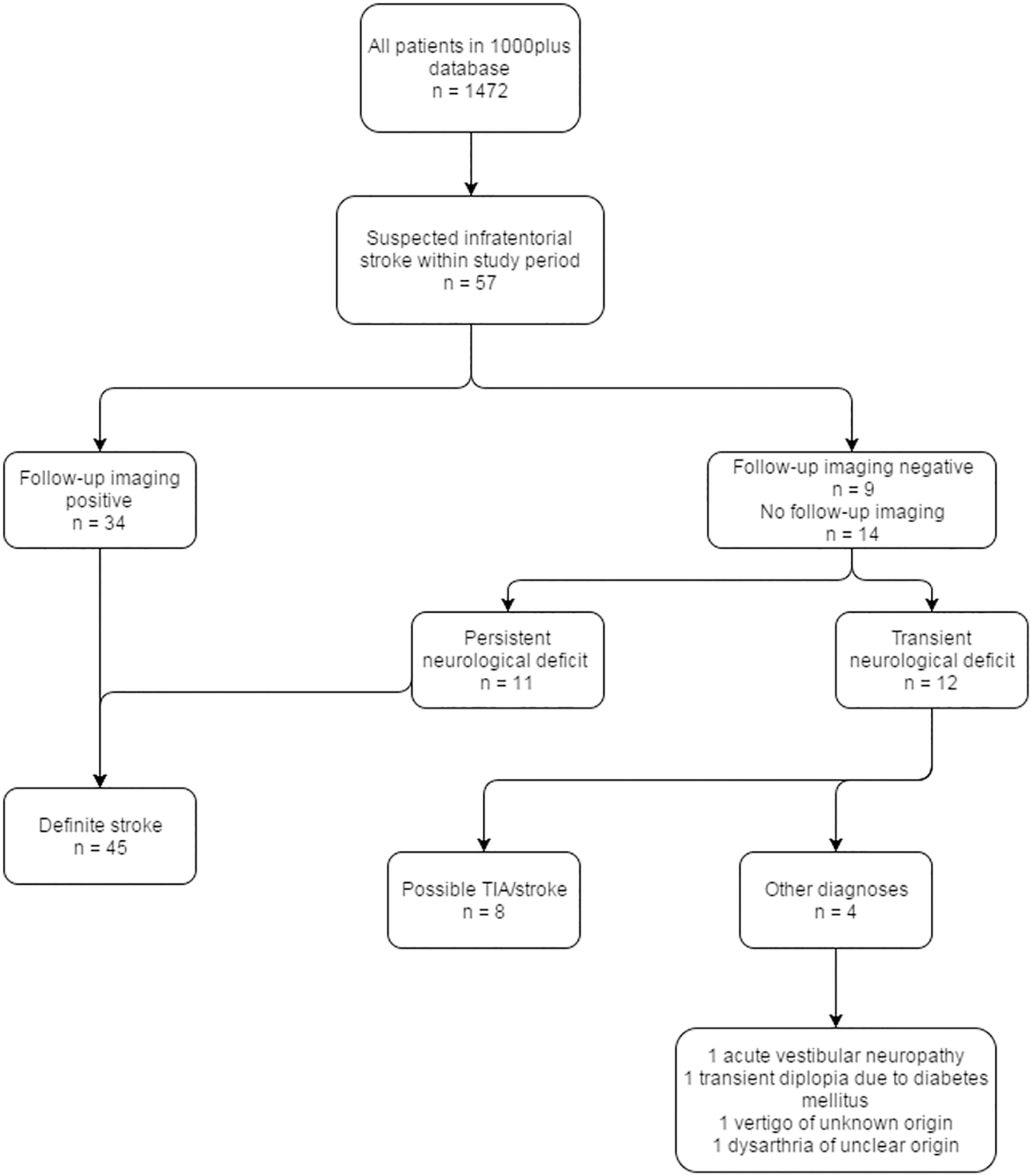

Fig 1. Flowchart of study participants.

doi:10.1371/journal.pone.0161416.g001

performed consecutively in the same scanning session without clinical intervention in between and their scanning parameters are shown in Table 1.

Although HR-DWI is highly sensitive to ischemia [6], it nevertheless suffers from false-negatives [11] and we therefore considered it to be an unsuitable reference standard in this study. Instead, each patient's final diagnosis was collected from the hospital records and discharge letters and was determined based on 1) clinical information, 2) follow-up MR imaging studies (FLAIR images performed at least one day and up to five days after the initial scan to confirm infarction and rule out alternative diagnoses), and 3) ancillary investigations including ECG, intra- and extracranial Doppler ultrasonography, and echocardiography. Patients received a final diagnosis of definite ischemic stroke if they had a persisting neurologic deficit at discharge or if they had imaging evidence of infratentorial infarction on follow-up MRI examinations. Similar to previous studies [4,5], this was used as the reference standard for all sensitivity calculations in this study.

Image analysis

After completion of the recruitment phase, four readers who were blinded to all clinical information, including each subject's final diagnosis, independently assessed the diffusion-weighted images. Two of them were senior, more experienced readers (a radiologist and a neuroradiologist with 7 and 14 years of stroke MRI experience respectively) and two were junior readers (a stroke researcher and a junior physician with 4 and 1.5 years of stroke MRI experience respectively). DWI images were randomly assigned with each reader assessing approximately half of the cases. Each image was assessed by both a senior and junior reader to calculate interobserver agreement.

The readers noted how many hyperintensities were visible on each diffusion-weighted image, the anatomical location of each hyperintensity, and whether it corresponded to an ischemic lesion or an artifact. Intraparenchymal hyperintensities that did not, in the readers' experience, correspond to an infarction but would likely cause some diagnostic confusion in the setting of suspected infratentorial stroke were considered relevant artifacts (see Fig 2 for an illustrative example). Typical susceptibility artifacts seen in the interface between tissues (see Fig 2), particularly around the temporal lobe, were not considered relevant artifacts in this study because they do not clearly lie within the brain parenchyma and are unlikely to be considered ischemic in practice.

Image signal-to-noise ratios were calculated by dividing the mean signal intensity within the brain on a single slice by the standard deviation of the signal intensity in a region of interest (ROI) outside the brain on the B0 images. In addition, we calculated the lesion percentage contrast-to-noise ratios (CNR) for 10 of the patients using the trace DWI images. After registering the images to a template, a ROI was placed within the acute infarct. A second ROI was placed in healthy-appearing tissue in the contralateral hemisphere in the case of cerebellar stroke and on the opposite side in brainstem strokes. The mean signal intensity in the lesion (SL) and the mean signal in the healthy tissue (SH) were extracted and percentage CNR was calculated as follows: 100 x (SL–SH)/SH [1].

Analysis

SPSS for Windows (Version 21; SPSS, Chicago, Ill) was used for statistical analysis.

Cohen's kappa, overall raw agreement, and proportions of specific agreement [12] between the DWI sequences on the presence or absence of ischemic lesions (based on the senior readers' judgement) were calculated and the intraclass correlation coefficient was used to evaluate the agreement on the number of ischemic lesions.

Table 1. Acquisition parameters for the DWI sequences.

Parameter	HR-DWI	LR-DWI	STEAM-DWI
Slice thickness (mm)	2.5	5	5
Number of slices	50	25	25
In-plane resolution (mm)	1.2 x 1.2	1.2 x 1.2	1.44 x 1.44
Matrix	192 x 192	192 x 192	160 x 120
Repetition time (s)	7.6	7.6	6.85
Echo time (s)	0.093	0.093	0.044
Diffusion-encoding gradient directions	6	6	6
b-value (s/mm^2)	1000	1000	1000
Number of averages	2	2	5
Acquisition time (s)	133	91	330

doi:10.1371/journal.pone.0161416.t001

Sensitivity of each DWI sequence to ischemia was calculated, including 95% confidence intervals. The sensitivities of each sequence were compared using McNemar's chi-square test.

In an exploratory analysis, we also calculated the sensitivity (and 95% confidence intervals) of each DWI sequence in patients presenting within 3 different time windows from stroke symptom onset to MR imaging ($\leq$ 12 hours, $>$ 12 $\leq$ 24 hours, and $>$ 24 hours).

Results

Participants

A total of 57 patients were recruited for the study (see Fig 1); 39 males and 18 females with a mean age of 68 years (range = 44 to 92 years). Median NIHSS was 2 (range = 0 to 12) on admission and 1 (range = 0 to 9) at discharge. Median time from symptom onset to imaging was 24 hours (range = 2 to 217 hours, IQR = 47 hours).

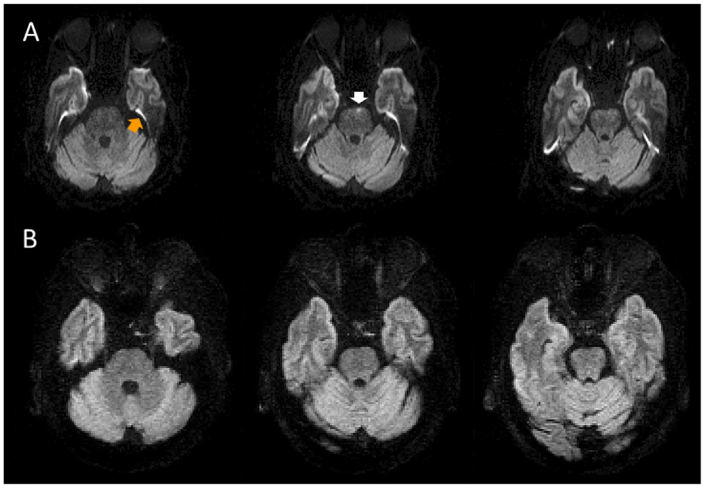

Fig 2. Artifacts on the DWI sequences. A) Example of artifacts on the high-resolution EPI-DWI (three consecutive slices shown). A typical susceptibility artifact is visible on the EPI-DWI (orange arrow)–note that such artifacts were ignored by the raters and are not the focus of this study. An intraparenchymal hyperintensity in the left pons (white arrow) is seen on a single slice. B) Neither of these artifacts is present on the STEAM-DWI.

doi:10.1371/journal.pone.0161416.g002

Presence and number of artifacts and ischemic lesions in the DWI sequences

At least one artifact was seen on 44/57 of the LR-DWI images (a total of 74 individual artifacts), 41/57 of the HR-DWI images (a total of 78 individual artifacts), and 1/57 of the STEAM-DWI images (a total of 1 artifact). Fig 2 shows examples of typical artifacts seen on the DWI sequences.

At least one hyperintensity due to ischemia was seen on 42/57 of the LR-DWI images (a total of 58 lesions), 46/57 of the HR-DWI images (a total of 71 lesions), and 44/57 of the STEAM-DWI images (a total of 60 lesions).

Agreement between DWI sequences on the presence of ischemia

STEAM-DWI agreed with the LR-DWI in 51/57 (89.5%) of cases (kappa = 0.72, $p<0.0001$), positive percent agreement (PPA) was 93% (95% CI = 86.8–97.8%) and negative percent agreement (NPA) was 78.6% (95% CI = 57.1–93%). STEAM-DWI agreed with the HR-DWI in 51/57 (89.5%) of cases (kappa = 0.68, $p<0.0001$), PPA was 93.3% (95% CI = 87.4–97.9%) and NPA was 75% (95% CI = 50–91.7%). LR-DWI agreed with HR-DWI in 53/57 (93%) of cases (kappa = 0.80, $p<0.0001$), PPA was 95.5% (95% CI = 90.2–99%) and NPA was 84.6% (95% CI = 66.7–96.8%). Fig 3 shows a representative example of agreement between the DWI sequences. Table 2 shows a cross-tabulation of these results.

The intraclass correlation coefficients for the number of ischemic lesions detected was 0.84 (95% CI = 0.74 to 0.9) for LR-DWI versus STEAM-DWI, 0.63 (95% CI = 0.45 to 0.76) for STEAM-DWI versus HR-DWI, and 0.77 (95% CI = 0.62 to 0.86) for LR-DWI versus HR-DWI.

Agreement between the senior and junior readers on the presence of hyperintensities corresponding to ischemia was calculated for the LR-DWI (kappa = 0.67, $p<0.0001$), HR-DWI (kappa = 0.55, $p<0.0001$), and STEAM-DWI (kappa = 0.62, $p<0.0001$) sequences.

Test results (sensitivity to ischemia)

Forty-five out of 57 patients had a confirmed final diagnosis of infratentorial infarction. Baseline imaging showed the presence of infarction in 39/45 (87%, 95% CI = 73.2–95%) of cases for LR-DWI, 42/45 (93%, 95% CI = 81.7–98.6%) of cases for HR-DWI, and 40/45 (89%, 95% CI = 76–96.3%) of cases for STEAM-DWI. The differences between sensitivities of STEAM-DWI and HR-DWI or STEAM-DWI and LR-DWI were not statistically significant ($p = 0.623$, $p = 0.99$, respectively).

Of the false-negative DWI images, true infarcts (confirmed by follow-up imaging or consistent with the patient's clinical deficit at hospital discharge) that were judged as artifacts by the readers were seen in 5 out of 6 of the LR-DWI, 2 out of 3 of the HR-DWI, and none of the STEAM images. In one patient, STEAM-DWI showed an ischemic lesion that was considered an artifact on the HR-DWI (see Fig 4).

Ischemic lesions were seen on the HR-DWI that were not detected on the STEAM-DWI sequence in three patients (see Fig 5). Table 3 shows a cross-tabulation of these results. Table 4 shows the sensitivity of each of the sequences to infarction stratified based on time from symptom onset to MR imaging.

Signal-to-noise and contrast-to-noise ratios

Image SNR (n = 53, mean +/- SD) was 78.7 +/- 16.0 for HR-DWI, 112.6 +/- 29.7 for LR-DWI, and 35.6 +/- 5.9 for STEAM-DWI. Lesion percentage CNR (n = 10, mean +/- SD) was 92.3% +/- 32.1% for HR-DWI, 73.7% +/- 27.4% for LR-DWI, and 43.5% +/- 12.5% for STEAM-DWI.

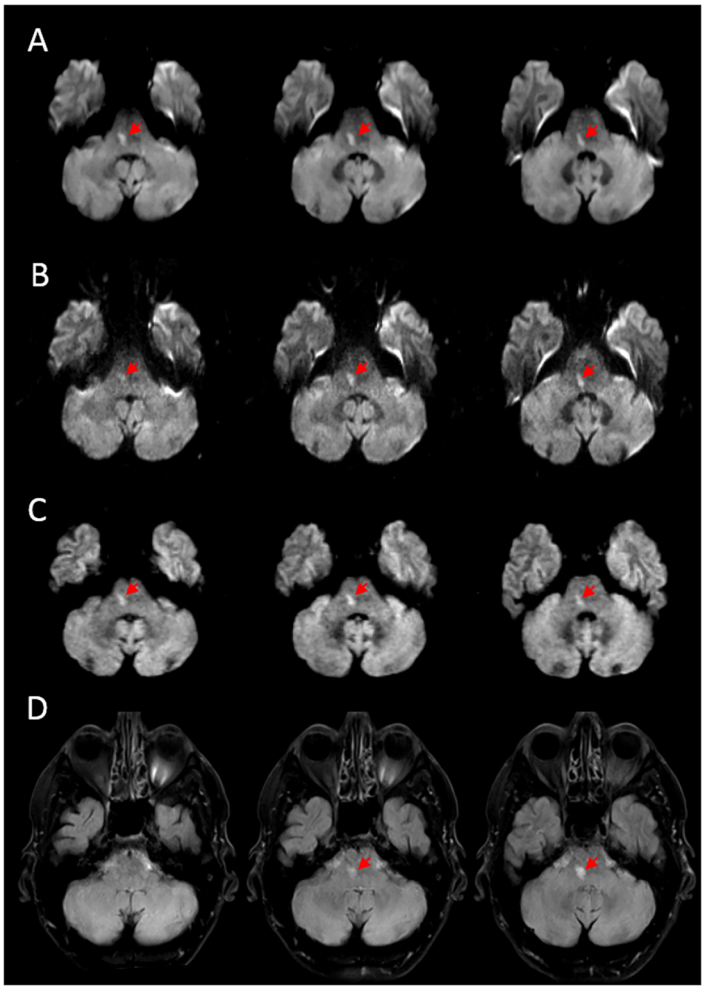

Fig 3. Representative example of agreement between DWI sequences for a patient studied 8 hours after onset of stroke symptoms. Both low- (A) and high-resolution (B) EPI-DWI show a hyperintensity in the right pons spanning three slices. C) STEAM-DWI also shows a hyperintensity in the right pons. D) FLAIR performed five days after baseline scans confirmed the presence of an infarct in the same location. Ischemic lesions are indicated by red arrows.

doi:10.1371/journal.pone.0161416.g003

Discussion

Diffusion-weighted imaging with stimulated echoes was used in some of the earliest studies investigating the detection of acute ischemia using MRI [13]. Since then, concerns about poor signal-to-noise ratios have overshadowed the potential advantages of this technique. To assess

Table 2. Cross-tabulation of STEAM-DWI versus HR-DWI and LR-DWI in the whole sample.

		HR-DWI		LR-DWI	
		Positive	**Negative**	**Positive**	**Negative**
STEAM-DWI	**Positive**	42	2	40	4
	Negative	4	9	2	11

Results of stimulated echo acquisition mode DWI (STEAM-DWI) compared to high-resolution EPI-DWI (HR-DWI) and low-resolution EPI-DWI (LR-DWI) sequences on presence or absence of ischemic lesions in the entire sample, regardless of final diagnosis.

doi:10.1371/journal.pone.0161416.t002

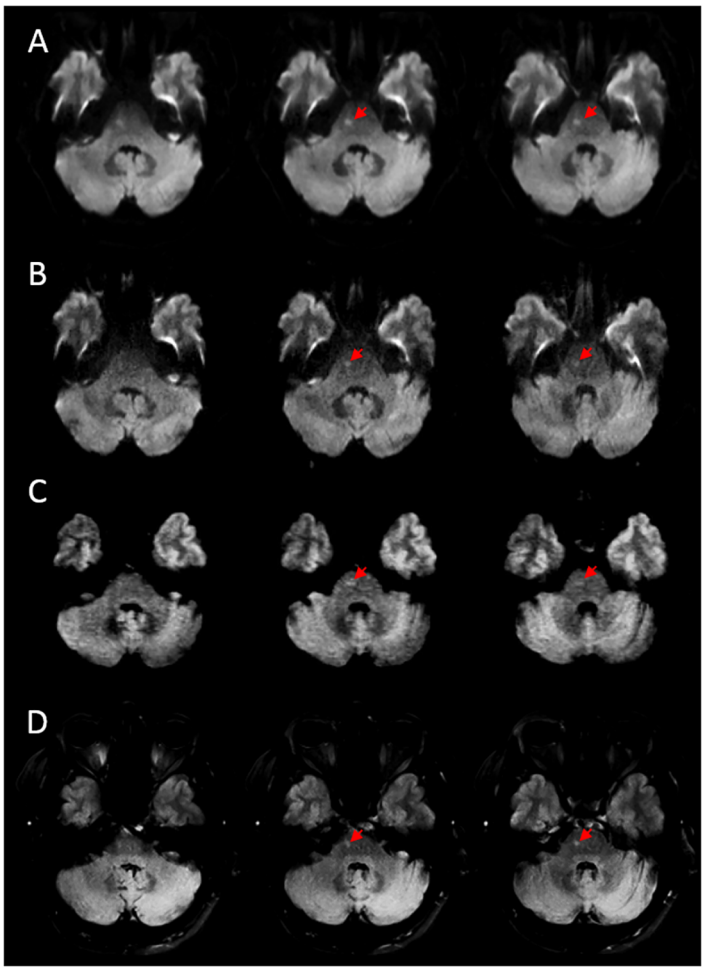

Fig 4. Example of disagreement between DWI sequences for a patient studied 19 hours after onset of stroke symptoms Both low- (A) and high-resolution (B) DWI show a hyperintensity in the right pons that was judged to be an artifact. C) The STEAM-DWI shows a hyperintensity in the right pons that was judged to be an ischemic lesion. D) FLAIR performed 5 days after baseline scans confirmed the presence of an infarct in the same location. Ischemic lesions are indicated by red arrows.

doi:10.1371/journal.pone.0161416.g004

the practical implications of these concerns, we determined the agreement between two EPI-based DWI sequences and a STEAM-based DWI sequence and compared their sensitivities to infratentorial ischemic stroke. We found good agreement between STEAM-DWI and EPI-based DWI sequences and similar sensitivity to ischemia in these patients.

On EPI sequences, susceptibility artifacts in areas adjacent to the temporal lobes and brainstem can appear as signal hyperintensities on diffusion-weighted images and can easily be confused for small, localized brainstem or cerebellar infarctions (see Fig 2). Our results show that such artifacts are far less frequent in STEAM-DWI than in either of the EPI-DWI sequences. Conversely, very small areas of ischemia can be mistaken for artifacts on EPI-DWI sequences–this happened in several cases in our study and substantially contributed to the false negative rates of these sequences (see Fig 4). Despite having a similar false-negative rate, no true ischemic lesion was misjudged as being artifact in the STEAM-DWI sequence. These results reaffirm the notion that the presence of DWI artifacts is of practical importance because it can hinder stroke diagnosis. Thus, using a sequence lacking these artifacts, either

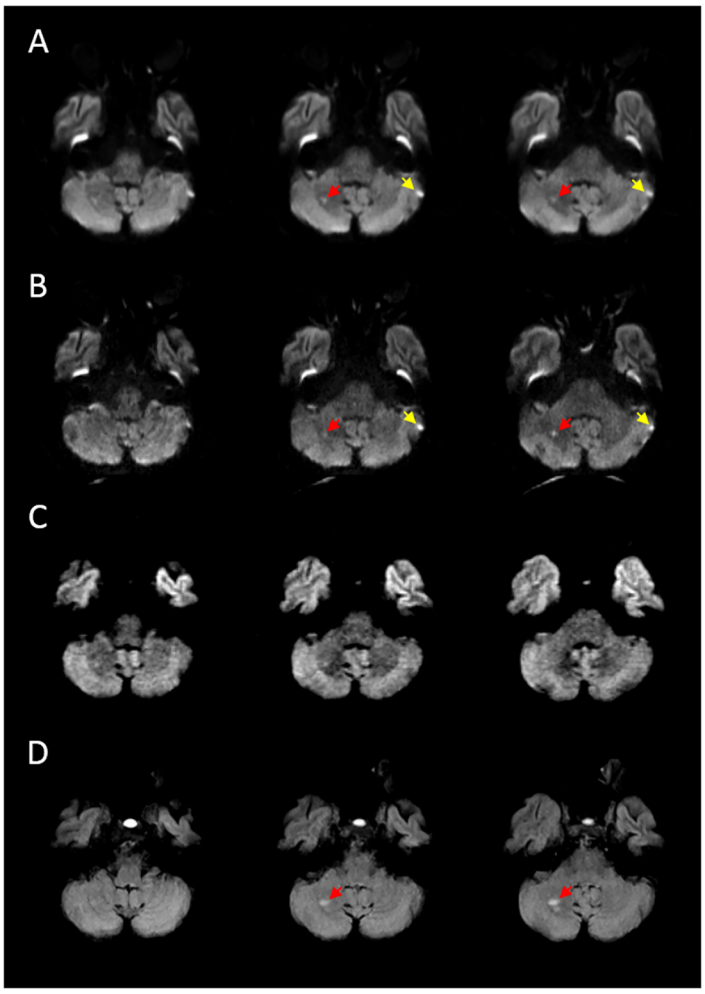

Fig 5. Example of disagreement between the DWI sequences. In this patient, MRI was performed 25 hours after the onset of stroke symptoms. Both low (A) and high-resolution (B) EPI-DWI show a hyperintensity (red arrows) in the right cerebellar lobe that was judged to be an ischemic lesion. Also note the hyperintensity in the periphery of the left cerebellar lobe (yellow arrows), which was judged to be an artifact. C) STEAM-DWI was judged as normal in this case. D) FLAIR performed 5 days after baseline scans confirmed the presence of an infarct in the same location.

doi:10.1371/journal.pone.0161416.g005

instead of conventional EPI-DWI or as an add-on, may be particularly helpful when the diagnosis is unclear.

STEAM sequences have inherently lower signal-to-noise ratios than spin-echo EPI sequences [14] yet we found good overall agreement between STEAM-DWI and both HR-DWI and

Table 3. Cross-tabulation of STEAM-DWI versus HR-DWI and LR-DWI in patients with confirmed stroke.

		HR-DWI		LR-DWI	
		Positive	**Negative**	**Positive**	**Negative**
STEAM-DWI	**Positive**	39	1	37	3
	Negative	3	2	2	3

Results of stimulated echo acquisition mode DWI (STEAM-DWI) compared to high-resolution EPI-DWI (HR-DWI) and low-resolution EPI-DWI (LR-DWI) sequences on presence or absence of ischemic lesions in patients with a confirmed final diagnosis of infratentorial stroke.

doi:10.1371/journal.pone.0161416.t003

Table 4. Sensitivity (and 95% CI) of DWI sequences to infarction (in patients with confirmed stroke) stratified by time from symptom onset to imaging.

	HR-DWI	LR-DWI	STEAM-DWI
≤12 hours (n = 12)	100% (73.5–100%)	100% (73.5–100%)	91.7% (61.5–99.8%)
>12 ≤ 24 hours (n = 15)	86.7% (59.5–98.3%)	80% (51.9–95.7%)	93.3% (68.1–99.8%)
>24 hours (n = 18)	94.4% (72.7–99.9%)	83.3% (58.6–96.4%)	83.3% (58.6–96.4%)

doi:10.1371/journal.pone.0161416.t004

LR-DWI for detecting ischemia. Agreement between the DWI sequences by itself is not necessarily an adequate measure of the diagnostic performance of STEAM-DWI in a clinical setting because it does not rule out the possibility that both sequences being compared mistakenly diagnosed the cases. We therefore used a final diagnosis of infratentorial infarction, collected from follow-up imaging and other clinical data as performed in previous similar studies [4,5], as a reference standard to compare the actual sensitivities of the different DWI sequences. Our results show that despite having substantially lower contrast-to-noise ratios than EPI-DWI, the rate of detection of ischemic lesions was similar between the sequences.

We found a false-negative rate of 7% for HR-DWI and 13% for LR-DWI. Both these values are substantially lower than those reported by Oppenheim et al. (31% for HR-DWI) and Benameur et al. (56% for LR-DWI) in infratentorial stroke [4,6]. However these authors only studied patients presenting within 24 hours of symptom onset, when hyperintensities on DWI may be less conspicuous [15,16] and used lower magnetic field strengths than our current study. Overall sensitivity to ischemia detection was similar between STEAM-DWI and LR-DWI in our study and the sensitivity of STEAM-DWI was only slightly lower than that of HR-DWI. These results suggest that STEAM-DWI is able to dependably detect infratentorial ischemia in the majority (89%) of cases.

It is important to note that despite overall sensitivity to ischemia being similar, the STEAM-DWI sequence detected fewer (n = 60) ischemic lesions than HR-DWI (n = 71). The data suggest that this difference is likely due to slice thickness, because the number of lesions detected by STEAM-DWI was similar to LR-DWI (n = 58). Small, scattered lesions may appear to coalesce or partially disappear due to partial volume effects associated with low spatial resolution in the slice-select direction [17]. The number and pattern of ischemic lesions provides clues to stroke etiology [18]. Therefore, an important technical improvement to the STEAM-DWI sequence would be to acquire thinner slices, potentially improving its detection of multiple lesions.

Our study has some limitations worth mentioning. Artifacts in the STEAM-DWI sequence could have been classified as ischemic lesions based on the readers' prior knowledge of the sequence's properties, erroneously inflating its sensitivity. Because of this, we interpreted our data under the assumption that it is unlikely for a hyperintensity located in the same location as the final infarct to be an artifact mistaken for true ischemia. We therefore looked at the results of each sequence not only in terms of presence or absence of ischemic lesions, but also based on lesion location (although this was only possible for patients with follow-up imaging). Assessing the specificity of the different sequences could also have helped clarify the effect of this potential bias. However, this could not be done in our study because, unless a clear alternative diagnosis is established, the lack of imaging evidence of an infarction does not reliably exclude infratentorial stroke [19–21].

The use of a clinical reference standard itself is a potential limitation because there is inherent inter-observer variability in the diagnosis of stroke [22,23], which is closely related to clinicians' experience [24]. Although our study was performed in a large center with considerable experience in managing stroke patients, the imperfect nature of the standard could have

affected our sensitivity estimates. Our strict definition of a definite stroke also meant that sensitivity estimates could only be calculated based on 45 patients in our sample of 57. This modest sample size was the result of the prolongation of our routine stroke MR protocol by the addition of two sequences, which could not be justified in every case. However, our study was sufficiently powered to detect a difference of 15% or more between the sensitivities of EPI-DWI and STEAM-DWI [25]. This minimum detectable difference is markedly less than is expected based on the differences in SNR and CNR between the two sequences.

Our sample mostly consists of patients with subacute stroke but 12 patients with a confirmed diagnosis of infratentorial stroke were scanned within 12 hours of symptom onset. A single infarct was missed by the STEAM-DWI sequence in this subgroup, although this subanalysis was exploratory and should be assessed in larger prospective studies. Taking into account the fact that DWI lesions tend to be less conspicuous in the early hours following symptom onset [15], particularly in posterior circulation stroke [4], assessing the performance of STEAM-DWI in very early stroke is crucial. In our current study, performing such a time-consuming protocol (with three separate DWI scans) in an early time window could not be justified.

In this study, we attempted to compensate for the inherently low SNR of the STEAM-DWI sequence by increasing the number of averages, which led to longer acquisition times (5.5 minutes). However, attempts at shortening the total acquisition time of the STEAM-DWI sequence while maintaining or improving SNR can be achieved by using head coils with more channels that better support parallel imaging [26]. Further technical improvements may be achieved by adopting concepts recently developed for real-time MRI [27]. Such ideas include the use of radial encoding strategies and pronounced data undersampling [28] in conjunction with iterative image reconstruction by regularized nonlinear inversion [29,30]. This may allow studies in earlier time windows to be done.

Conclusions

The results of our study show that STEAM-DWI suffers far less from artifacts mimicking ischemia than conventional EPI-DWI sequences. The sensitivity of STEAM-DWI to the presence of ischemia is similar to that of the best currently available MRI sequence used for this purpose, HR-DWI. With further technical development, STEAM-DWI may become a useful replacement or add-on to conventional DWI sequences in cases of suspected infratentorial stroke.

Supporting Information

S1 Fig. STandards for the Reporting of Diagnostic accuracy studies (STARD) checklist.
(DOC)

Author Contributions

Conceptualization: MH CK WS KV JF KDM JBF.

Data curation: AK CK.

Formal analysis: AK.

Funding acquisition: JBF.

Investigation: MH KV CK JBF.

Methodology: PB MH.

Project administration: CK KV WS JBF.

Resources: JBF JF KDM.

Supervision: JF JBF.

Visualization: AK.

Writing - original draft: AK.

Writing - review & editing: AK MH CK WS PB KV KDM JF JBF.

References

1. González RG, Schaefer PW, Buonanno FS, Schwamm LH, Budzik RF, Rordorf G, et al. Diffusion-weighted MR imaging: diagnostic accuracy in patients imaged within 6 hours of stroke symptom onset. Radiology. Radiological Society of North America; 1999; 210: 155–62. doi: 10.1148/radiology.210.1.r99ja02155
2. Warach S, Dashe JF, Edelman RR. Clinical outcome in ischemic stroke predicted by early diffusion-weighted and perfusion magnetic resonance imaging: a preliminary analysis. J Cereb Blood Flow Metab. 1996; 16: 53–59. doi: 10.1097/00004647-199601000-00006 PMID: 8530555
3. Lovblad K, Laubach H, Baird A, Curtin F, Schlaug G, Edelman R, et al. Clinical experience with diffusion-weighted MR in patients with acute stroke. AJNR Am J Neuroradiol. 1998; 19: 1061–1066. Available: http://www.ajnr.org/content/19/6/1061.abstract PMID: 9672012
4. Oppenheim C, Stanescu R, Dormont D, Crozier S, Marro B, Samson Y, et al. False-negative Diffusion-weighted MR Findings in Acute Ischemic Stroke. AJNR Am J Neuroradiol. 2000; 21: 1434–1440. Available: http://www.ajnr.org/content/21/8/1434.full PMID: 11003275
5. Chalela JA, Kidwell CS, Nentwich LM, Luby M, Butman JA, Demchuk AM, et al. Magnetic resonance imaging and computed tomography in emergency assessment of patients with suspected acute stroke: a prospective comparison. Lancet (London, England). 2007; 369: 293–8. doi: 10.1016/S0140-6736(07)60151-2
6. Benameur K, Bykowski JL, Luby M, Warach S, Latour LL. Higher Prevalence of Cortical Lesions Observed in Patients with Acute Stroke Using High-Resolution Diffusion-Weighted Imaging. AJNR Am J Neuroradiol. 2006; 27: 1987–1989. Available: http://www.ajnr.org/content/27/9/1987.long PMID: 17032880
7. Merboldt K-D, Hänicke W, Bruhn H, Gyngell ML, Frahm J. Diffusion imaging of the human brainin vivo using high-speed STEAM MRI. Magn Reson Med. 1992; 23: 179–192. doi: 10.1002/mrm.1910230119 PMID: 1734178
8. Nolte UG, Finsterbusch J, Frahm J. Rapid isotropic diffusion mapping without susceptibility artifacts: whole brain studies using diffusion-weighted single-shot STEAM MR imaging. Magn Reson Med. 2000; 44: 731–6. Available: http://www.ncbi.nlm.nih.gov/pubmed/11064408 PMID: 11064408
9. Rieseberg S, Merboldt K-D, Küntzel M, Frahm J. Diffusion tensor imaging using partial Fourier STEAM MRI with projection onto convex subsets reconstruction. Magn Reson Med. 2005; 54: 486–90. doi: 10.1002/mrm.20572 PMID: 16032668
10. Hotter B, Pittl S, Ebinger M, Oepen G, Jegzentis K, Kudo K, et al. Prospective study on the mismatch concept in acute stroke patients within the first 24 h after symptom onset-1000Plus study. BMC Neurol. 2009; 9: 60. doi: 10.1186/1471-2377-9-60 PMID: 19995432
11. Hotter B, Kufner A, Malzahn U, Hohenhaus M, Jungehülsing GJ, Fiebach JB. Validity of negative high-resolution diffusion-weighted imaging in transient acute cerebrovascular events. Stroke. Lippincott Williams & Wilkins; 2013; 44: 2598–600. doi: 10.1161/STROKEAHA.113.001594
12. Cicchetti D V, Feinstein AR. High agreement but low kappa: II. Resolving the paradoxes. J Clin Epidemiol. Pergamon; 1990; 43: 551–558. doi: 10.1016/0895-4356(90)90159-M
13. Warach S, Chien D, Li W, Ronthal M, Edelman RR. Fast magnetic resonance diffusion-weighted imaging of acute human stroke. Neurology. 1992; 42: 1717–23. Available: http://www.ncbi.nlm.nih.gov/pubmed/1513459 PMID: 1513459
14. Frahm J, Merboldt K, Hänicke W, Haase A. Stimulated echo imaging. J Magn Reson. 1985; 64: 81–93. doi: 10.1016/0022-2364(85)90033-2
15. Schlaug G, Siewert B, Benfield A, Edelman RR, Warach S. Time course of the apparent diffusion coefficient (ADC) abnormality in human stroke. Neurology. Lippincott Williams & Wilkins; 1997; 49: 113–119. doi: 10.1212/WNL.49.1.113

16. Lansberg MG, Thijs VN, O'Brien MW, Ali JO, de Crespigny AJ, Tong DC, et al. Evolution of Apparent Diffusion Coefficient, Diffusion-weighted, and T2-weighted Signal Intensity of Acute Stroke. AJNR Am J Neuroradiol. 2001; 22: 637–644. Available: http://www.ajnr.org/content/22/4/637.long PMID: 11290470

17. Molyneux PD, Tubridy N, Parker GJM, Barker GJ, MacManus DG, Tofts PS, et al. The effect of section thickness on MR lesion detection and quantification in multiple sclerosis. Am J Neuroradiol. American Society of Neuroradiology; 1998; 19: 1715–1720. Available: http://www.ncbi.nlm.nih.gov/pubmed/9802495

18. Caso V, Budak K, Georgiadis D, Schuknecht B, Baumgartner RW. Clinical significance of detection of multiple acute brain infarcts on diffusion weighted magnetic resonance imaging. J Neurol Neurosurg Psychiatry. 2005; 76: 514–8. doi: 10.1136/jnnp.2004.046383 PMID: 15774438

19. Makin SDJ, Doubal FN, Dennis MS, Wardlaw JM. Clinically Confirmed Stroke With Negative Diffusion-Weighted Imaging Magnetic Resonance Imaging. Stroke. 2015; 46: 3142–3148. doi: 10.1161/STROKEAHA.115.010665 PMID: 26419965

20. Watts J, Wood B, Kelly A, Alvaro A. Stroke syndromes associated with DWI-negative MRI include ataxic hemiparesis and isolated internuclear ophthalmoplegia. Neurol Clin Pract. 2013; 3: 186–191. doi: 10.1212/CPJ.0b013e318296f288

21. Nalleballe K, Jadeja N, Bollu P, Onteddu S. DWI Negative Stroke: Learning Points For Imaging In Acute Stroke (P1.037). Neurology. 2015; 84: P1.037.

22. Shinar D, Gross CR, Mohr JP, Caplan LR, Price TR, Wolf PA, et al. Interobserver Variability in the Assessment of Neurologic History and Examination in the Stroke Data Bank. Arch Neurol. American Medical Association; 1985; 42: 557–565. doi: 10.1001/archneur.1985.04060060059010

23. Hatano S. Variability of the diagnosis of stroke by clinical judgement and by a scoring method. Bull World Health Organ. World Health Organization; 1976; 54: 533–40. Available: http://www.ncbi.nlm.nih.gov/pubmed/1088403

24. Hand PJ, Haisma JA, Kwan J, Lindley RI, Lamont B, Dennis MS, et al. Interobserver Agreement for the Bedside Clinical Assessment of Suspected Stroke. Stroke. Lippincott Williams & Wilkins; 2006; 37: 776–780. doi: 10.1161/01.STR.0000204042.41695.a1

25. Beam C. Strategies for Improving Power in Diagnostic Radiology Research. AJR. 1992; 159: 631–637. PMID: 1503041

26. Parikh PT, Sandhu GS, Blackham KA, Coffey MD, Hsu D, Liu K, et al. Evaluation of image quality of a 32-channel versus a 12-channel head coil at 1.5T for MR imaging of the brain. AJNR Am J Neuroradiol. 2011; 32: 365–73. doi: 10.3174/ajnr.A2297 PMID: 21163877

27. Uecker M, Zhang S, Voit D, Karaus A, Merboldt K-D, Frahm J. Real-time MRI at a resolution of 20 ms. NMR Biomed. 2010; 23: 986–94. doi: 10.1002/nbm.1585 PMID: 20799371

28. Zhang S, Block KT, Frahm J. Magnetic resonance imaging in real time: advances using radial FLASH. J Magn Reson Imaging. 2010; 31: 101–9. doi: 10.1002/jmri.21987 PMID: 19938046

29. Uecker M, Hohage T, Block KT, Frahm J. Image reconstruction by regularized nonlinear inversion—joint estimation of coil sensitivities and image content. Magn Reson Med. 2008; 60: 674–82. doi: 10.1002/mrm.21691 PMID: 18683237

30. Uecker M, Zhang S, Frahm J. Nonlinear inverse reconstruction for real-time MRI of the human heart using undersampled radial FLASH. Magn Reson Med. 2010; 63: 1456–62. doi: 10.1002/mrm.22453 PMID: 20512847

5 Curriculum Vitae

Mein Lebenslauf wird aus datenschutzrechtlichen Gründen in der elektronischen Version meiner Arbeit nicht veröffentlicht.

My curriculum vitae is not published in the electronic version of my dissertation for data protection reasons.

6 Complete List of Publications

An up-to-date list is available here: https://orcid.org/0000-0003-1752-4305

6.1 Peer-reviewed original research articles

Khalil AA, Ostwaldt AC, Nierhaus T, Ganeshan R, Audebert HJ, Villringer K, Villringer A, Fiebach JB. Relationship between Changes in the Temporal Dynamics of the Blood-Oxygen-Level-Dependent Signal and Hypoperfusion in Acute Ischemic Stroke. *Stroke*. 2017;48:925–931.

Villringer K, Sanz Cuesta BE, Ostwaldt AC, Grittner U, Brunecker P, **Khalil AA**, Schindler K, Eisenblätter O, Audebert H, Fiebach JB. DCE-MRI blood–brain barrier assessment in acute ischemic stroke. *Neurology*. 2017;88:433–440.

Khalil AA, Hohenhaus M, Kunze C, Schmidt W, Brunecker P, Villringer K, Merboldt KD, Frahm J, Fiebach JB. Sensitivity of diffusion-weighted STEAM MRI and EPI-DWI to infratentorial ischemic stroke. *PLoS One*. 2016;11:e0161416.

Jadavji NM, Farr TD, Lips J, **Khalil AA**, Boehm-Sturm P, Foddis M, Harms C, Füchtemeier M, Dirnagl U. Elevated levels of plasma homocysteine, deficiencies in dietary folic acid and uracil-DNA glycosylase impair learning in a mouse model of vascular cognitive impairment. *Behav. Brain Res.* 2015;283:215–226.

Ibrahim MM, **Khalil AA**, Khan UA. Offspring sex ratios among male tobacco smokers in Khartoum, Sudan. *J Pak Med Assoc* 2012; 62: 1045–1049.

6.2 Book chapters

Khalil AA. Positron emission tomography. In: Vonk J, Shackelford T, editors. *Encyclopedia of Animal Cognition and Behavior*. Springer; 2017. p. 1–6.

Khalil AA. Blindsight. In: Vonk J, Shackelford T, editors. *Encyclopedia of Animal Cognition and Behavior. Springer*; 2017. p. 1–3.

6.3 Preprints

Lakens D, Adolfi FG, Albers C, Anvari F, Apps MA, Argamon SE, Assen MA van, Baguley T, Becker R, Benning SD, Bradford DE, Buchanan EM, Caldwell A, Calster B van, Carlsson R, Chen S-C, Chung B, Colling L, Collins G, Crook Z, Cross ES, Daniels S, Danielsson H, DeBruine L, Dunleavy D, Earp BD, Ferrell JD, Field JG, Fox N, Friesen A, Gomes C, Grange JA, Grieve A, Guggenberger R, Harmelen A-L Van, Hasselman F, Hochard KD, Hoffarth MR, Holmes NP, Ingre M, Isager P, Isotalus H, Johansson C, Juszczyk K, Kenny D, **Khalil AA**, Konat B, Lao J, Larsen EG, Lodder GM, Lukavsky J, Madan C, Manheim D, Gonzalez-Marquez M, Martin SR, Martin AE, Mayo D, McCarthy RJ, McConway K, McFarland C, Nilsonne G, Nio AQ, Oliveira CL de, Parsons S, Pfuhl G, Quinn K, Sakon J, Saribay SA, Schneider I, Selvaraju M, Sjoerds Z, Smith S, Smits T, Spies JR, Sreekumar V, Steltenpohl C, Stenhouse N, Świątkowski W, Vadillo MA, Williams M, Williams D, Xivry J-JO de, Yarkoni T, Ziano I, Zwaan R. Justify Your Alpha: A Response to "Redefine Statistical Significance." *PsyArXiv*. 2018;1–18.

6.4 Selected conference abstracts

Khalil, AA, Kirilina, E., Villringer, K., Villringer, A., Fiebach, J.B. The Effect of Scan Length on the Assessment of Cerebral Perfusion Using Resting-state Functional MRI: A Comparison Between Sequences in Acute Stroke, in: *ASNR 55th Annual Meeting 2017. Long Beach, CA* (oral presentation)

van Sloten, I., Galinovic, I., Boehm-Sturm, P., Kellner, E., **Khalil, AA**, Fiebach, J.B. Comparison of microvasculature between young and elderly individuals as well as subjects with pronounced leukoaraiosis using MRI vessel size imaging, in: *European Stroke Organisation Conference 2017*. SAGE Publications, Prague (poster)

Khalil, AA, Villringer, K., Filleböck, V., Rocco, A., Fiebach, J.B., Villringer, A. Non-invasive monitoring of reperfusion in ischemic stroke using BOLD signal delay, in: *European Stroke Organisation Conference 2017*. SAGE Publications, Prague (poster)

Galinovic, I., Kochova, E., **Khalil, AA**, Villringer, K., Piper, S.K., Fiebach, J.B. The mismatch between cerebral blood flow and Tmax predicts the quality of collaterals in acute ischemic stroke, in: *European Stroke Organisation Conference 2017*. SAGE Publications, Prague. (poster)

Villringer, K., Sanz Cuesta, B.E., Ostwaldt, A.-C., Grittner, U., Brunecker, P., **Khalil, AA**, Schindler, K., Eisenblätter, O., Audebert, H.J., Fiebach, J.B. DCE-MRI blood-brain barrier

assessment in acute ischemic stroke, in: *JCBFM (BRAIN 2017 Conference)*. SAGE Publications, Berlin (poster)

Khalil, AA, Kirilina, E., Villringer, K., Fiebach, J.B., Villringer, A. Perfusion maps based on temporal blood-oxygen-level-dependent signal delays are driven by alterations in low frequency oscillations between 0.01 and 0.1 Hz, in: *JCBFM (BRAIN 2017 Conference)*. SAGE Publications, Berlin (poster)

Khalil AA, Mueller S, Foddis M, Dirnagl U, Fiebach JB, Villringer A, Boehm-Sturm P. Time shift analysis of resting-state functional MRI data in a mouse model of focal cerebral ischemia: preliminary results. *ESMRMB 2016, 33rd Annual Scientific Meeting*, Vienna (oral presentation)

Khalil AA, Kirilina E, Nierhaus T, Villringer K, Villringer A, Fiebach JB. Independent component analysis of resting-state hemodynamics in acute stroke: a new approach for identifying hypoperfusion. *ESMRMB 2016, 33rd Annual Scientific Meeting*, Vienna (oral presentation)

Khalil AA, Villringer K, Rocco A, Fiebach JB, Villringer A. Vessel recanalization and recovery of resting BOLD signal delay in acute ischemic stroke. *European Stroke Organisation Conference 2016, Barcelona* (poster)

Hu JJY, **Khalil AA**, Ganeshan R, Villringer K, Villringer A, Fiebach JB. Validation of a novel, automated perfusion lesion-detection algorithm in acute ischemic stroke. *European Stroke Organisation Conference 2016, Barcelona* (poster)

Fan A, **Khalil AA**, Fiebach JB, Villringer A, Zaharchuk G, Villringer K, Gauthier C. Noninvasive Assessment of Quantitative Oxygen Extraction Fraction Ischemic Stroke by MRI Susceptibility: A Pilot Study. *ASNR 54th Annual Meeting 2016, Washington DC* (oral presentation)

Villringer K, **Khalil AA**, Brunecker P, Nolte C, Villringer A, Fiebach JB. Inverse PWI/DWI Mismatch is a Typical Feature of Acute Subcortical Ischemic Stroke. *International Stroke Conference 2016, Los Angeles, CA*;47: ATP47–ATP47 (poster)

Khalil AA, Mueller S, Foddis M, Fiebach JB, Villringer A, Boehm-Sturm P, Bedside-to-bench Translation: Lessons from MR Imaging in Acute Stroke. *Berlin Institute of Health Symposium 2016: Exploring Systems Medicine, Berlin* (poster)

Khalil AA, Ostwaldt AC, Nierhaus T, Audebert HJ, Villringer K, Villringer A, Fiebach JB. Diagnostic and volumetric agreement between BOLD signal delay and bolus-tracking MRI on perfusion deficits in acute ischaemic stroke. *European Stroke Organisation Conference 2015, Glasgow* (poster)

Khalil AA, Ostwaldt AC, Nierhaus T, Nave AH, Koch P, Villringer K, Villringer A, Fiebach JB. Assessing cerebral perfusion by measuring BOLD signal delay in acute ischaemic stroke: A volumetric comparison with bolus-tracking MRI. *Thrombolysis, Thrombectomy, and Acute Stroke Therapy 2014, Mannheim* (poster)

Jadavji NM, Farr TD, Lips J, **Khalil AA**, Boehm-Sturm P, Harms C, Foddis M, Füchtemeier M, Dirnagl U. Folic acid deficiency increases plasma homocysteine and results in learning deficits in a mouse model of chronic hypoperfusion. *8th Symposium on Neuroprotection and Neurorepair 2014, Magdeburg* (poster)

Khalil AA, Galinovic I, Brunecker P, Villringer K, Fiebach JB. The effect of slice thickness on perfusion imaging in posterior circulation stroke. *ESMRMB 2012, 30th Annual Congress. Toulouse* (poster).

7 Acknowledgments

Over the past few years, I have been very fortunate to meet and be surrounded by a wonderful group of people. The following scarcely does justice to my gratitude.

For funding me throughout my time as a PhD student, I thank the NeuroCure Cluster of Excellence and the Max Planck Institute for Human Cognitive and Brain Sciences.

My mentor, **Prof. Dr. med. Jochen B. Fiebach**, made the start of my research career possible. He took me in for a lab rotation as a (slightly lost) master's student and since then has provided me with the ideal balance of unwavering support and independence. The faith he has in his students and employees is inspiring.

I am grateful to the current and former members of AG CSB Neuroradiology, especially Dr. med. Kersten Villringer (who always had my back), Dr. Ivana Galinovic (without whom I might have never known the world of stroke MRI), Dr. rer. medic. Peter Brunecker (for inspiring me to learn how to program), Dr. Ralf Mekle (for our many thought-provoking discussions), and my predecessor Dr. Ann-Christin Ostwaldt (for being a great co-worker and friend).

I owe a great deal to **Prof. Dr. Arno Villringer** – I left every one of our Wednesday meetings brimming with newfound confidence and ideas. His brilliant charm, wit, and genuine concern for his students helped keep me going.

I am indebted to many people at the Berlin School of Mind & Brain, in particular Dr. rer. medic. Till Nierhaus, who patiently spent many hours walking me through analysis scripts. Overall, the PhD life might have seemed a bit dull if it were not for the many vibrant conversations about science I had with Dr. rer. nat. Smadar Ovadia-Caro over coffee.

Alongside Jochen and Arno, my appreciation goes to **Dr. Philipp Boehm-Sturm**, the third of my supervisors. He kept me focused on reaching my goals while ensuring I kept a watchful eye on my workload, and reminded me to kick back and relax every now and then.

For forcing me to think about things I never thought I needed to think about, in ways I never thought possible, my gratitude goes to my students (to Yiing in particular, for our political discussions and for encouraging me to try new things – mostly food). And for giving me a hobby that has turned into a passion, my profound thanks go to the entire team of the *Charité NeuroScience (CNS) newsletter* – especially Marietta, Apoorva, and Constance.

For all the laughs and delightful times we shared together over the past few years, my heartfelt thanks go to my dearest friends, Meron and Mari.

Finally, I will always owe all my successes, past and future, to my family – especially my parents and sisters. Their love, patience, and encouragement is worth more than the entire world to me.